1993

Water Quality Impacts of Naturals Riparian Grasses Part 2: Modeling Effects of Channelization on Sediment Trapping

S. P. Inamdar
University of Kentucky

B. J. Barfield
University of Kentucky

D. I. Carey
Kentucky Geological Survey

Alex W. Fogle
Kentucky Geological Survey

WATER QUALITY IMPACTS OF NATURALS RIPARIAN GRASSES:

PART II: MODELING EFFECTS OF CHANNELIZATION ON SEDIMENT TRAPPING.

by

S.P Inamdar, Graduate Assistant
Agricultural Engineering Department

B. J. Barfield, Emeritus Professor
Agricultural Engineering Department

D.I. Carey, Hydrologist
Kentucky Geological Survey

A.W. Fogle, Hydrologist III
Kentucky Geological Survey

University of Kentucky
Lexington, Kentucky 40506

Water Resources Research Institute
University of Kentucky
Lexington, Kentucky
June, 1993

ABSTRACT

A methodology is developed to determine expected sediment trapping in riparian vegetative filter strips considering channelization of flow. The framework consists of defining the channel network stochastically, with deposition/detachment in each channel being modeled deterministically. The two approaches were then combined to develop a model which could predict expected trapping efficiencies for vegetative filters under known field conditions. The model was then extended to include conditions such as rainfall on the filter so as to make it applicable to generic field situations.

Field and laboratory studies were conducted to collect and estimate data to develop and evaluate the model. Sediment concentrations were measured for natural vegetative filters located on a slope of 8.7%, subjected to inflows from upslope bare soil plots. Surface elevations were measured for the filter. Flow networks and channel shapes were defined by applying the digital elevation model to the micro-relief data. Actual distributions and standard fitted distributions for channel flows and channel shapes were developed.

Model evaluation was done for selected values of Manning's n to give predicted filter trapping efficiencies within 2% of the observed, indicating model validity. Sensitivity analysis was conducted using the general model and the fitted probability distributions.

CHAPTER II.1

INTRODUCTION

The Soil Conservation Service has recommended the use of riparian vegetative filter strips as a Best Management Practice (BMP) to control non-point source pollution (NPS). Vegetative filter strips (VFS) are bands of planted or indigenous vegetation, situated between pollutant source areas and receiving waters, which are intended to remove sediment and other pollutants from surface runoff (Heatwole et al., 1991). Several studies as summarized in Part I of this report have shown that vegetative filter strips are effective in preventing and controlling pollution due to sediment, nutrients and organics (Dillaha et al., 1986,87,88).

Dillaha et al. (1986) evaluated the long term effectiveness of VFS, using on farm surveys on a quarterly basis. As a result of this study a number of problems regarding the long term effectiveness of the filter strips were identified. It was found that most VFS were implemented without a site specific design criteria and thus failed to achieve the desired pollutant reduction goals. VFS installed in highly sloping regions were particularly observed to be less effective than those on flatter slopes, due to channelization which occurred, leaving the major portion of the filter inactive and ineffective. Under short term periods (1-3 years) VFS's in the flatter regions were more effective as the flow was more spread out and traveled through the filter as shallow flow. After a couple of years, however, sediment accumulation was observed at the upslope leading edge of the filter which caused the runoff to travel parallel to the width of the filter and enter the filter as concentrated flow at a low point on the filter. These channels that formed in the filter had a greater depth of flow and higher velocity as compared to shallow overland flow and also provided less opportunity for infiltration.

An additional problem in the effectiveness of the VFS used in controlling non-point pollution is that they are not being required on ephemeral channels. The proposed regulations require VFS along perennial streams depicted on the most recent USGS 7 1/2 -minute topographic quadrangle maps. Since most surface runoff collects in ephemeral drainageways that are not shown on the USGS maps, much of the non-point source flow will be unaffected by the proposed regulation (Heatwole et al., 1991).

The US Soil Conservation Service is updating the National Conservation Practice Standard for VFS to overcome some of its limitations (Dillaha, 1989). The proposed standards define VFS as vegetated areas that are *"designed"* to remove sediment, nutrients, pathogens, organic materials, pesticides, and other contaminants from surface runoff by filtration, deposition, infiltration, adsorption, decomposition and volatilization. The key word here is *"design"*, which implies that natural VFSs are not necessarily suitable for every site, and their width and location shall be a function of the local site conditions and hydrology. Such considerations for design may involve determining optimum dimensions for filter strips, primarily taking into account channelization of flow through the filter.

A number of design models such as GRASFIL (Hayes et al., 1979) have been developed in the past to simulate short term behavior of filter strips. First estimates from these models are good enough for initial installation and functioning of the filters. However, since the models assume uniform shallow overland flow they overpredict sediment trapping under channelized flow conditions. To meet the growing needs for site specific design of vegetative filters to be used for state conservation programs, a model was needed which could accurately predict trapping efficiency of filters under all site conditions such as varying slopes, runoff and degree of channelization.

To fill that need, an effort is made in this research to represent the channelization of flow in grass filters and to determine the trapping efficiency of the filter of given dimensions under conditions where channelized flow occurs over all or part of the filter. The channel network is represented and analyzed using stochastic methods, whereas sediment deposition/detachment is modeled using physically based fundamental approaches. The stochastic approach consists of determining the probable number of channels forming down the filter length, along with the distribution of flows and channel shapes associated with each channel. The deterministic approach physically defines the sediment transport and deposition phenomenon on a channel/rill by channel/rill basis. These two approaches are then combined to determine the expected trapping. The approach here is not to define the actual physical system as observed on the field, but to get a probablisitic description of it. The specific objectives of this research were

- Develop a methodology to represent the channelization of flow in the filter using stochastic approaches.
- Incorporate this methodology into a model which can be effectively used for site specific design of riparian filter strips to be installed on upland drainage channels.
- Validate the methodology used in the model and its ability to determine expected trapping efficiencies for filters using experimental observations from field grass studies.
- Extend the model scope for generic conditions (such as rainfall on the filter), thus enhancing its applicability and use as a general grass filter model encompassing all expected criteria.

CHAPTER II.2

RELATED RESEARCH

Introduction

Modeling soil detachment/deposition has been accomplished with both empirical and fundamental methods.

Sediment Deposition and Detachment

Basic Principles and Concepts

Soil erosion and sedimentation occur as a result of three unique and interrelated processes: soil detachment, transport, and deposition. Modeling of these combined processes typically starts with the mass continuity equation for sedimentation.

$$D_r+D_i=\frac{\partial q_s}{\partial x} \qquad \text{(II.2.1)}$$

where q_s is the sediment load, x is the distance downslope, D_r is the rate of detachment/deposition in the rills and D_i is the rate of detachment/deposition in the interill areas. For non-steady state conditions the equation is given as

$$D_r+D_i=\frac{\partial q_s}{\partial x}+\rho_s\frac{\partial cy}{\partial t} \qquad \text{(II.2.2)}$$

where ρ_s is the mass density of sediment particles, c is the concentration of sediment in the flow and y is the flow depth varying with time t.

In the development of the above two equations deposition or detachment was assumed to be independent of the sediment in the flow. Meyer and Monke (1965) proposed that detachment and deposition are not independent of the sediment load but are rather influenced by it. Hence, considering the interdependence between detachment and deposition, Foster and Meyer(1972) then further defined detachment by the equation

$$D_r=C_1(T_c-q_s) \qquad \text{(II.2.3)}$$

where T_c is the transport capacity, q_s is the sediment load and C_1 is a coefficient. Foster and Meyer proposed that as the runoff impinges on an erodible layer and has sufficient transport capacity, detachment will be initiated. This detachment will increase down the slope until a point in which the sediment load in the flow is equal to the transport capacity. Any reduction in the transport capacity beyond that point due to changes in the flow hydraulics will lead to deposition of the sediment. Thus

transport capacity and sediment load are the limiting conditions that govern deposition or detachment.

This phenomenon can be written in equation form as

$$\frac{D_r}{C_1 T_c} + \frac{q_s}{T_c} = 1.0 \qquad \text{(II.2.4)}$$

or

$$\frac{D_r}{D_{rc}} + \frac{q_s}{T_c} = 1.0 \qquad \text{(II.2.5)}$$

where D_{rc} is the maximum detachment rate also defined as the term $C_1 T_c$ in equation II.2.4. Equation II.2.5 shows that when the sediment load q_s in the flow is zero then D_r the detachment rate equals the maximum detachment rate D_{rc}, and when D_r is zero the sediment load equals the transport capacity.

Channel Network Processes in Riparian Vegetation

Use of digital elevation models for determining channel networks has recently received attention. In this method, preferential flow paths are determined based on microtopographic data and soil properties. One such comprehensive model was developed at the USGS Data Center by Jenson and Dominque (1988). This model takes a raster grid of topographic elevations, divides the surface into cells of equal dimensions, and then delineates the preferential flow paths and their watershed boundaries. The major operations involved in this analysis are filling topographic depressions, flow direction delineation, and spatial computation of flow accumulation. For a detailed description of the model the reader is referred to Storm et al. (1991).

Rill Detachment and Deposition in Channels

In contrast to the limited knowledge base for models available to represent the rill network patterns, channel erosion and deposition on a individual rill basis has been studied extensively. As discussed earlier, the three processes that govern channel process are soil detachment, transport, and deposition. The three processes are discussed in the following sections

Detachment: Detachment occurs when the flow shear stresses acting along the rill boundary exceed the critical binding forces by which the soil particles are held together. The rate of soil detachment can be expressed as

$$D_{rc} = \alpha (\overline{\tau} - \tau_c)^b \qquad \text{(II.2.6)}$$

where D_{rc} is the maximum detachment rate, $\overline{\tau}$ is the average flow shear stress along

the rill boundary, τ_c is the critical shear stress needed to detach the soil particle and a,b are constants. The average shear τ_o can be determined based on the knowledge of the channel shape and the hydraulic radius, or

$$\overline{\tau} = \gamma RS \qquad \text{(II.2.7)}$$

where γ is the specific weight of the water, R is the hydraulic radius and S is the bed slope of the rill. Critical shear stress for rills can be determined using the Shield's diagram (1936). Shield's diagram uses spatially averaged dimensionless shear stress, and particle Reynold's number calculated at the bed as parameters. The original Shield's diagram was extended by Mantz (1977) to be applicable for particles of smaller diameter. Typical critical shear stress values available for agricultural soils range from 1 to 30 Pa (N/m^2).

Sediment Transport: Sediment transport may occur in the form of wash load, bed load, or suspended load. Wash load consists of particle sizes much smaller than sizes present in the bulk of the parent bed material. Bed load consists of sediment particles moving along the bed of the channel by saltation, rolling, or sliding. Suspended load consists of particles in the smaller size range of bed load material which move for a appreciable period of time in suspension.

A number of models have been developed to simulate sediment transport in rills and overland flow. Their application to any field situation is subject to the conditions present. The most common bed load transport models being used are the Yalin Model (1963) and the unit stream power model developed by Yang (1973). Other total load models include the Acker's and White (1973), Laursen (1958), and Einstein's bed load equations (1950).

Yalin's bed load equation and Einstein's calibrated total load equation are most commonly used to model sediment transport through grass media and shallow flow. Einstein's equation was modified by Tollner et al. (1982) to consider the total sediment load transport through grass filter strips. This is the relationship used in this model and is discussed later in the chapter.

Rill Deposition: Deposition of sediment load in rills occurs when the sediment load exceeds transport capacity. Deposition occurs with coarser particles settling preferentially compared to the finer sized sediment. Deposition has been given by Foster and Meyer (1972) as the excess of sediment load over transport capacity, or

$$D_p = \alpha (T_c - q_s) \qquad \text{(II.2.8)}$$

where α is the deposition coefficient and other terms are as defined before. Tollner el al. (1982) also developed an exponential deposition model applicable to filter strips. The Tollner et al. model is discussed later in this chapter.

Rill Detachment/Deposition Models: A number of rill detachment/deposition models have been developed for small shallow channels, including Foster and Lane's

model (1980, 1983), KYERMO (Hirschi and Barfield, 1988a), Mossaad and Wu (1984), CREAMS, and finally WEPP. A stochastic approach towards determining rill detachment/deposition was utilized by Lewis et al. (1991) in PRORIL, as discussed in the following section.

PRORIL: PRORIL is a model for determining expected values of rill erosion on bare soil on moderate slopes (Lewis et al., 1991) using a probabilistic approach. Rill networks were represented with a stochastic methodology, and rill erosion modeled using physically based fundamental methods on a individual rill basis. This has similarities to the approach used in this report to model channel networks in riparian vegetation.

In PRORIL an analysis of sediment yield from a bare plot was accomplished by discretizing the slope into segments of equal length, and the storm duration into equal time steps. Sediment continuity was assumed across the complete length of the plot. Total rill erosion for each segment was determined and summed down the plot to give the total yield at the end of the plot.

Rill density 'n' for each segment was determined with its associated probability p(n). Probability values for channel density were determined from binomial distributions fitted to observed rill density data. Given the rill density in a section, the distribution of flow rates 'q' and the conditional probability 'p(q|n)' associated with each of them was determined. Conditional probability values were derived from fitting Weibull distribution to flow rates computed from data. Knowing the rill density, rill flow rates, and their respective pdf's, an algorithm was developed to determine the expected detachment/deposition across the plot or

$$E(D_p) = \sum_{i=1}^{imax} p(n_i)\, n_i \left[\sum_{j=1}^{jmax} p(q_j | n_i)\, h(q_j) \right] \qquad \text{(II.2.9)}$$

where $h(q_j)$ is the detachment/deposition associated with each flow rate $E(D_p)$ is the expected deposition across the segment, $p(n_i)$ is the probability of n rills on the slope segment, $p(q_j|n)$ is the conditional probability of flowrate q given n rills. Total incoming sediment load was partitioned between all the flow rates in proportion of the ratio of the individual flow rate to the total runoff across the section.

Rill detachment was modeled using Foster and Lane's approach, with detachment rate in the rill given as

$$D_{r[j]} = D_{rc[j]} \left[1 - \frac{q_{[j]}}{T_{c[j]}} \right] \qquad \text{(II.2.10)}$$

where D_r is the average detachment rate at the middle of the segment T_c is the sediment load and transport capacity at the middle of the segment respectively, and

q_j is the flow rate for which detachment is being determined. Deposition was modeled using the equation

$$D_{r[j]} = \alpha_{[j,b]} (T_{c[j,b]} - q_{s[j,b]}) \qquad \text{(II.2.11)}$$

where D_r is the deposition rate for flow j and particle type b at the middle of the segment and α is the deposition coefficient.

Transport capacity in the rills was determined using Yalin's equation as a function of rill shape with modification for particle size distribution (Foster, 1982). Rill shape corresponding to every discrete flow rate was considered as rectangular and updated after deposition or detachment.

Previous Grass Filter Modeling Approaches

A number of models exist that determine sediment trapping in vegetative filter strips. Most of these models assume shallow uniform across the width of the filter strip, thus neglecting the effects of channelization of flow through the filter.

GRASFIL

GRASFIL was developed at the University of Kentucky by conducting basic studies of sediment transport in laboratory flumes utilizing artificial vegetative media with carefully controlled geometries (Tollner et al., 1976, 1982,; Barfield et al., 1979) and projecting these results to the field scale via a physically based model (Hayes et al., 1979, 1984).

According to Hayes et al. (1979), as sediment laden flow impinges on a grass filter, its velocity is retarded, and its transport capacity is reduced. If the transport capacity is less than the inflow sediment load, sediment is deposited at the inlet of the filter media. This deposition causes the channel slope to increase with a resulting increase in velocity and sediment transport capacity down the deposition face.

Further, Hayes et al. (1979) divided the filter into four zones for calculating trapping as shown in Figure II.2.1. The length of each zone varies with time as the sediment is deposited down the filter strip. In zone A(t), deposition of sediment has occurred till the top of the media is reduced and essentially all the incoming load is transported down to the next zone. Sediment deposition in zone B(t) occurs in the form of a triangular wedge with the incoming sediment being uniformly deposited along the slope. The slope of the deposition wedge is referred to as the equilibrium slope. In zones C(t) and D(t), the assumption is made that the tractive force is less than the critical value for the original channel bed. In section C(t), sufficient sediment has been deposited on the original channel bed so that all the surface irregularities are filled allowing the sediment to be transported as bedload. In zone D(t) insufficient material has been deposited on the bed to fill the irregularities, thus, all the sediment reaching the bed is trapped.

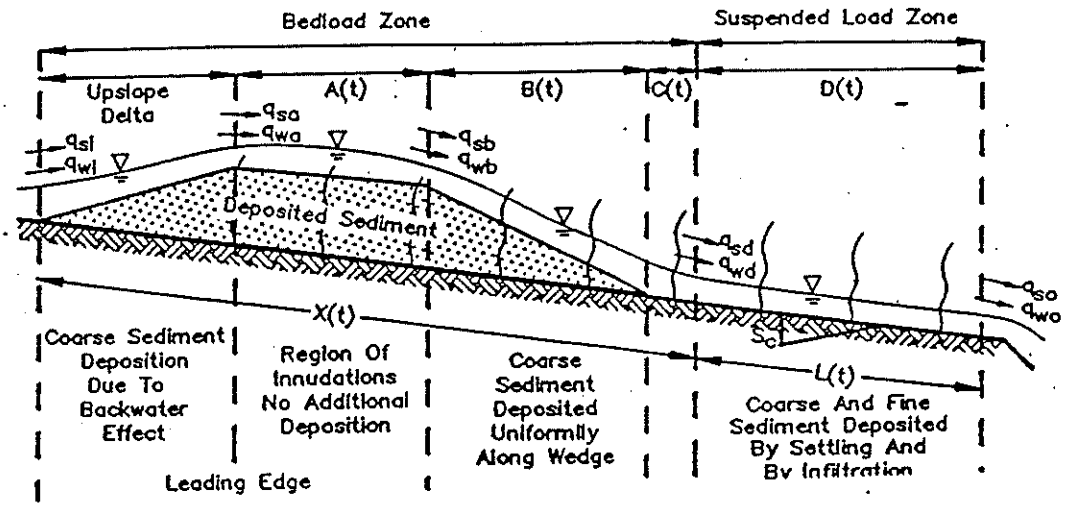

Figure II.1: Illustration of Zones of Sediment Transport for GRASFIL (Source: Barfield et al., 1979).

Infiltration is assumed to be primarily occurring in zone D(t) with the amount of infiltration equal to the difference between the inflow and outflow from the filter.

The assumptions made in the development of the GRASFIL model are:

- Erect, non-submerged filter elements.
- Incoming sediment load is greater than the transport capacity of the flow through the filter; hence, deposition of sediment in the filter is the dominant phenomenon.
- The travel velocity of the sediment is considered the same as that of the overland flow.

Development of Equations for Sediment Trapping

In GRASFIL, flow depth and velocity must first be calculated. Tollner et al. (1979) showed that flow velocity in the VFS can be determined using a modified form of Manning's equation given as

$$V_m = \left(\frac{1.5}{Xn}\right) R_s^{\frac{2}{3}} S_c^{\frac{1}{2}} \ (ft/\sec) \qquad \text{(II.2.12)}$$

where xn is calibrated value of Manning's roughness, S_c is the slope of the channel and R_s is the spacing hydraulic radius, given as

$$R_s = \frac{(S_s\ d_f)}{(2d_f + S_s)} \qquad \text{(II.2.13)}$$

where d_f is the depth of flow and S_s is the spacing between the media. The flow per unit width is given as

$$q_w = V_m d_f \qquad \text{(II.2.14)}$$

Equation II.2.12 and II.2.14 can be solved for flow depth and velocity. Given these values, sediment trapping can be determined in zone D(t) as described below. In zone D(t) the layer of litter on the bed has not been filled completely; thus, bedload transport is zero. Trapping efficiency in this zone was assumed in GRASFIL to be directly dependent on the number of times a particle could settle to the bed and inversely proportional to the flow Reynolds number (Tollner et al., 1976). Hence, the trapping efficiency in this zone was given as

$$T_s = \frac{(q_{sd} - q_{so})}{q_{sd}} = e^{(-1.05 \times 10^{-3} R_e^{0.32} N_f^{0.91})} \qquad \text{(II.2.15)}$$

where q_{sd} is the sediment load entering D(t), q_{so} is the sediment load exiting D(t), R_e is the Reynolds flow number given by

$$R_e = \frac{V_m R_s}{\nu} \qquad \text{(II.2.16)}$$

where ν is the kinematic viscosity and N_f is the fall number given by

$$N_f = \frac{V_s L(t)}{V_m d_f} \qquad \text{(II.2.17)}$$

where V_s is the settling velocity, and L(t) is the total length of the zone varying with time.

Zone C(t) is the zone where there is sufficient deposition to allow bed load transport but not enough deposition to alter the bed slope. Tollner et al. (1982) developed a calibrated version of the Einstein bedload function to predict sediment transport in zone C(t) or

$$\psi = 1.08\,(\phi)^{-0.28} \qquad \text{(II.2.18)}$$

where Ψ is the Einstein's shear intensity given as

$$q_{ss} = \frac{q_{si} + q_{sd}}{2} \qquad \text{(II.2.25)}$$

S_{et} was calculated in a trial and error solution technique using the equation

$$q_{ss} = \frac{K(R_{sb}\, S_{et})^{3.57}}{d_p^{2.07}} \qquad \text{(II.2.26)}$$

where R_{sb} is the spacing hydraulic radius on the deposition wedge and K is a constant given as $6.242 \times 10^7 \times SG(SG - 1)^{3.07}$

Hayes et al. (1979) extended the above equations to consider non-homogenous sediment. The form of most equations remains the same with the difference being that the particle size distribution is updated at different points down the filter.

The particle size distribution was divided into three particle size classes or

- Coarse Fraction: Particle Sizes greater than 0.037 mm.
- Medium Fraction (silt): Particle sizes in the range of 0.037 to 0.004 mm.
- Fine Fraction (clay): Less than 0.004 mm.

Particles greater than 0.037 mm in size were assumed to be trapped in the sediment wedge. Mean particle size for each class was determined based on weight. Coarser particle were assumed to deposit at the leading edge of the filter (zone A and B of the filter). The medium and the fine size sediment was assumed to be trapped in the lower portion of the filter (zone C and D). Particle size distribution was recalculated at three points down the filter length as shown in the Figure II.2.2.

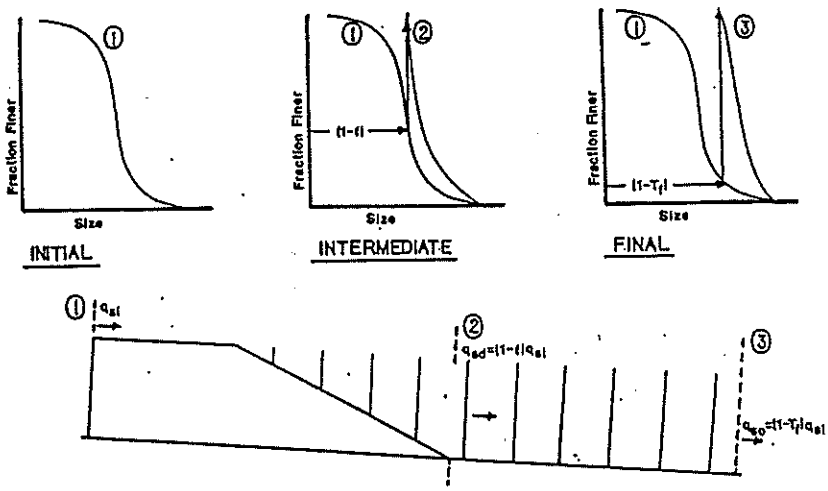

Figure II.2.2. Locations at which the particle size distributions are recalculated in GRASFIL (Source: Hayes et al. 1979).

The modified equation for total trapping considering a non homogenous sediment distribution was then given by

$$T=\left(\left[f+f_T^L(1.0-f) \right] (1.0-fr^1) + f_T^M(fr^1-fr^o) + f_T^F fr^o \right) \qquad \text{(II.2.27)}$$

where f is the fraction of large particles trapped in the deposition wedge, f_T^L, f_T^M, f_T^F are fractions trapped in the in zone D(t) of large, medium and fine particles respectively, fr^1 is a fraction finer than 0.037 mm and fr^o is the fraction finer than 0.004 mm.

Modeling Sediment Trapping in VFS Using CREAMS Equations

Flanagan et al. (1989) demonstrated that CREAMS (USDA, 1980) could be used to predict sediment delivery through vegetative filter strips. For development of the equations, the filter strip was assumed to be located downslope of a cultivated soil plot of known length as illustrated in Figure II.2.3.

The sediment load in the grass strip can be given as a sum of the deposition and lateral inflow of sediment from interrill erosion or

$$G=\int (D_F+D_L)\,dx \qquad \text{(II.2.28)}$$

where G is the sediment load, D_F is deposition in rills, and D_I is lateral flow of sediment into a rill.

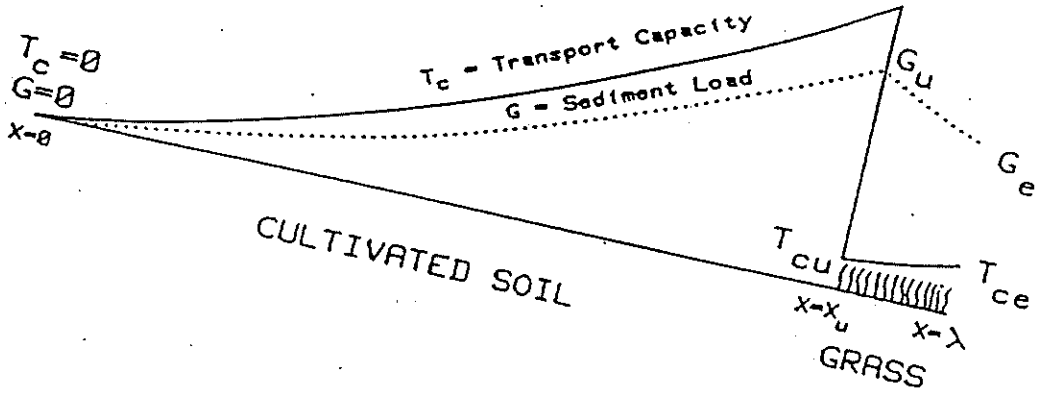

Figure II.2.3. Transport Capacity and Sediment Load on a Slope with a Grass Filter (Source: Flanagan et al., 1989).

The deposition in the filter strip based on the CREAMS model was given as (Flanagan et al., 1989)

$$D_F=[\frac{\phi}{(1+\phi)}](\frac{dT_c}{dx}-D_L)[1-(\frac{x_u}{x})^{1+\phi}]+D_u(\frac{x_u}{x})^{1+\phi} \qquad \text{(II.2.29)}$$

where D_F is the deposition rate, $\Phi = \beta V_f/\sigma$ is a measure of depositability, β is turbulence factor, V_f is particle fall velocity, σ is the excess rainfall rate, T_c is the transport capacity of flow at x, x is position downslope, D_L is lateral inflow of sediment from interrill erosion, x_u is length of upper segment and D_u is the deposition rate at x_u.

Using the above two equations and assuming D_L equal to zero, Flanagan showed that

$$G=[\frac{\phi}{1+\phi}](\frac{dT_c}{dx})[x+(\frac{x_u^{1+\phi}}{\phi})x^{-\phi}]-D_u(\frac{x_u^{1+\phi}}{\phi})x^{-\phi}+C \qquad \text{(II.2.30)}$$

where C is the constant of integration.

The transport capacity was calculated using the Yalin equation, which in CREAMS was assumed to be a linear function of x or

$$T_c=(\frac{dT_c}{dx})x \qquad \text{(II.2.31)}$$

Hence, the transport capacity T_{cu} (transport capacity of incoming flow) was computed as

$$T_{cu}=(\frac{dT_c}{dx})x_u \qquad \text{(II.2.32)}$$

Since G_u (sediment load in incoming flow) was known, the value of D_u was computed as

$$D_u=(\frac{\phi}{x_u})(T_{cu}-G_u) \qquad \text{(II.2.33)}$$

Using these values, the constant of integration was found to be equal to zero. Hence the sediment load at the end of the strip (at $x=\lambda$) was given as

$$G_e=[\frac{1}{1+\phi}]T_{ce}[\phi+x_u{*}^{1+\phi}]-(T_{cu}-G_u)(x_u{*})^{\phi} \qquad \text{(II.2.34)}$$

where

Experiments were performed by Flanagan et al. (1989) in which they observed that the above developed equations predicted the sediment trapping in VFS satisfactorily.

RUSLE (Revised Universal Soil Loss Equation): Erosion/Deposition Equations for Filter Strips

Erosion/deposition equations were developed in RUSLE for predicting sediment trapping in grass buffer strips/natural riparian vegetative filter strips. These equations were primarily developed for determining the Support Practice Factor for strip cropping and grass strips alternately situated on an hillslope. The erosion/deposition equations were developed based on the fundamental erosion concepts developed by Renard and Foster (1983). The model calculates erosion, sediment transport and deposition in the filter strip considering the following conditions

- Erosion along the full length of the strip
- Deposition on the upper edge of the strip and erosion at the lower end.
- Deposition for the full length of the strip.

Condition I: Erosion Along the Full Length of the Filter Strip

The sediment load exiting the strip in this case is given as

$$g_i = g_{i-1} + \xi_i \zeta_i (x_i^n - x_{i-1}^n) \qquad \text{(II.2.41)}$$

where ξ is an erosion factor that is proportional to the erosion rate, ζ is transport capacity factor and x is the normalized distance downslope (absolute distance/slope length). Here n has a value of 1.0, but in case of rill formation in the VFS, n = 1.5.

Condition II: Deposition as Well as Erosion in the Strip

Deposition in a filter strip occurs when the sediment load in the flow is greater than the transport capacity of flow. If the filter length is sufficiently long, a point might be reached in the filter strip where the transport capacity equals the sediment load. In such a case erosion will occur beyond this point. The basic equation used to model deposition is given by

$$D = \left(\frac{\phi}{x}\right)(T - g) \qquad \text{(II.2.42)}$$

where T is the transport capacity and g is sediment load, computed based on the approach taken in WEPP

$$T = x\zeta \tag{II.2.43}$$

where ζ is a transport capacity factor, and Φ is parameter describing depositability of the sediment. RUSLE's approach for calculating Φ for a sediment mixture was similar to that taken in WEPP. The effective value of Φ for three particle sizes (primary clay, primary silt and small aggregate) is expressed by

$$\phi_e = e^{\left[\frac{(\sum f_i \ln \phi_i)}{3}\right]} \tag{II.2.44}$$

where f is the fraction of sediment composed of class k. Hence the deposition at upper edge of the filter strip is given by

$$D_{i-1} = \left(\frac{\phi_e}{x_{i-1}}\right)\left(\zeta_i x_{i-1} - g_{i-1}\right) \tag{II.2.45}$$

The position in the filter strip where deposition ends and erosion starts is given by

$$x_e = x_{i-1}\left\{1 - \left[\frac{(1+\phi)}{\phi}\right]\left(\frac{D_{i-1}}{\zeta_i}\right)\right\}^{\frac{1}{1+\phi}} \tag{II.2.46}$$

At this point the sediment load should be equal to the transport capacity of the flow. Beyond this point downslope, additional sediment may be produced due to erosion. Hence the sediment yield at the bottom of the strip is the sum of the transport capacity at x_e and the erosion beyond that point or

$$g_i = \zeta_i x_e + \xi_i \left(x_i^n - x_e^n\right) \tag{II.2.47}$$

Condition III: Deposition Along the Full Length of the Filter Strip

In case the x_e value is greater than the length of the filter, no erosion will occur within the filter. The deposition over the entire strip in that case is given as per CREAMS or,

$$D_i = \left[\frac{\phi_e}{1+\phi_e}\right]\zeta_i\left[1 - \left(\frac{x_{i-1}}{x_i}\right)^{1+\phi_e}\right] + D_{i-1}\left(\frac{x_{i-1}}{x_i}\right)^{1+\phi_e} \tag{II.2.48}$$

The sediment load exiting from the strip in this case is

$$g_i = T_i - \frac{D_i x_i}{\phi_e} \tag{II.2.49}$$

Thus using these equations, sediment deposition and sediment yield can be determined.

Summary and Conclusions

Modeling of sediment trapping in grass filters to date has been restricted to a deterministic approach. Present models, such as GRASFIL, assume a uniformly distributed shallow flow across the width of the filter. Though such an approach gives a good initial estimate for constructed vegetative filter strips (sufficiently leveled) it overpredicts sediment trapping for naturally occurring vegetative filter strips located along upland drainage channels. These models overpredict deposition because the flow in these filters is typically concentrated in channels. Channelized flow occurs in grass filters when flow concentrates at low points between the sediment deltas, formed due to previous deposition. Channelization is greatly accentuated for grass filters on moderate to high slopes leading to a significant part of the filter being inactive.

Models presently available accurately predict trapping of grass filters on low slopes (in absence of channelized flow); however, a model is needed that can simulate and predict sediment trapping in riparian grass filters on moderate or high slopes considering channelization of flow. The model needs to meet the following criteria

- A true representation of the channelized flow for a given type and slope of the grass filter should be made. This objective could only be attained using a stochastic approach.
- Changes in channelization patterns and their respective flow rate distributions for changes in filter slopes should be modeled.
- Changes in channel patterns and flow rates with time (storm event duration), should be dynamic in nature.
- Initial channel/rill shapes should be modeled and modified for possible deposition/detachment.
- Detachment/deposition in channels without any previous deposition and with previous deposition should be modeled.
- Infiltration in grass filters and its changes with time and deposition should be modeled.

CHAPTER II.3

MODEL DEVELOPMENT

Introduction

The objective of this study was to develop a model that could predict sediment trapping in natural grass filters where flows have become channelized. Since it would be virtually impossible to determine and model the actual channel networks in a grass filter, a stochastic approach will be utilized. Channel networks and flow rates will be defined stochastically and deposition/detachment defined using a deterministic approach. The combination of these two approaches will yield expected trapping values for a given group of statistically similar filter plots.

Analysis of Stochastic and Dependent Parameters

The approach used in this research was to define the stochastic parameters, analyze their probability distributions, and develop an algorithm in which they could be combined with a physically based sediment deposition algorithm. The combination provides an estimate of the expected deposition in filter strips.

Given a population of filter plots, the major difference which sets them (filter plots) apart is their unique flow networks. Flow networks can be defined by channel densities and the distribution of flows in each of the channels and their respective channel shapes. Hence, channel density, channel flows and the channels shapes are the governing parameters that need to be modeled stochastically.

The number of channels at any segment down the filter is governed by the microtopography of the filter. The number may vary along the length of the filter and also with flow duration. Flows in each of these channels is a result of partitioning of the total incoming runoff into the total number of channels across the section. Hence, channel density and total runoff at any segment controls the flow in each of the channels. Since channel density varies with flow duration, flow rate distribution also varies with flow duration.

For a given flow rate there also exists an associated channel shape which changes with the development (detachment/deposition) of the channel. At any given instant, channels with similar flows may have different shapes associated with them. In each of these unique channels, sediment can be transported with deposition/detachment or transport depending on the channel flow and the channel shape. Modeling of deposition/detachment or transport can be accomplished given the flow rate and channel shape.

Measurement of changes in channel density, flow, and shape with time is difficult, if not impossible, with present technology. It is not possible at this time to represent stochastic variation of these parameters with time. The stochastic distribution of these parameters will be based on the conditions at the end of the

storm event, assuming that a steady state condition is being represented. Hence, by neglecting the variability with time, in essence we are assuming that the flow duration in each of the channels is equal to the length of the storm event. In other words, all channels were formed at the start of the storm event.

Channel density at any segment is the number of channels across the section. In grass filters, an infinite number of channels may represent a shallow sheet flow situation, and fewer channels may represent channelized flow. If 'n' is the number of channels at a section, the probability density for 'n' will be given as f(n). If 'q' is the flow in any one of the 'n' channels the conditional probability distribution associated with 'q' will be given as f(q|n), where q|n is the flow q given n rills/channels. Channel shape can be represented by a parameter 'W/D' where W is the top width of the channel and D is the channel depth. Hence, the conditional probability distribution associated with a channel shape or W/D value for a flow q can be given as f(W/D|q) where W/D|q is the shape W/D for a unique flow q.

Given the above stochastic distribution, the dependent parameters that could be modeled physically are

- Transport capacity (T_c)
- Deposition ($-D_p$)
- Detachment ($+D_p$)
- Sediment load and particle size distribution

Transport capacity (T_c) is the ability to transport sediment in each rill/channel. Deposition is given as D_p and is predicted with a negative sign. A positive D_p value is considered as detachment. In the model, detachment/deposition is computed per unit length and determined for each rill/channel in the segment.

Development of the Sediment Trapping Algorithm and Sediment Routing Down the Filter

Consider a segment on a filter plot with a given flow network. The deposition (D_p) or trapping across the segment at any point downslope is the summation of the deposition/trapping occurring in each of the individual channels, represented in this approach as the expected value of deposition. Considering sediment continuity the sediment exiting a segment can be given by

$$Q_s^{m+1} = Q_s^m + E\left(D_p^{m+1/2}\right) \cdot \Delta x \qquad \text{(II.3.1)}$$

where Q_s^{m+1} is the total sediment load exiting the segment, Q_s^m is the sediment load entering the segment, $E(D_p^{m+1/2})$ is the deposition in all the channels at half length of the segment and Δx is the segment length. Thus the total deposition/trapping for the plot would be then the sum of deposition over all the segments down the plot. In

using a discrete approach like this, it is assumed that parameters used to define the fundamental methods; such as critical tractive force, depth to non-erodible layer, Manning's n, slope and bulk density; are constant over the length of a given segment.

The stochastic approach to predicting $E(D_p)$ is similar to that used in an earlier study by Lewis et al. (1991) in which detachment/deposition was predicted in rills formed on bare soil. Lewis et al. showed that the average deposition across a segment with n rills is given by

$$E(D_p|n) = n \cdot \overline{(D_r|n)} \qquad \text{(II.3.2)}$$

where $E(D_p|n)$ is the total expected deposition in all the n rills, n is the number of rills across the section and $\overline{(D_r|n)}$ is the average deposition in each of the n rills. Using fundamentals of conditional probability Lewis et al. further showed that

$$E(D_p) = \int n \int D_r(q) \cdot f(q|n) \cdot f(n)\, dq\, dn \qquad \text{(II.3.3)}$$

where $D_r(q)$ is the detachment/deposition occurring in the rill for a given flow rate, $f(q|n)$ is the conditional probability distribution function for q given n and f(n) is the probability distribution function for n. Lewis et. al. (1991) discretized the above equation to give

$$E(D_p) = \sum_{i=1}^{imax} p(n_{[i]})\, n_{[i]} \left[\sum_{j=1}^{jmax} p(q_{[j]}|n_{[i]})\ D_r(q_{[j]}) \right] \qquad \text{(II.3.4)}$$

where $E(D_p)$ is the expected deposition across the slope width, $n_{[i]}$ is the number of rills and $p(n_{[i]})$ the probability associated with n rills, $q_{[j]}$ is the flow rate and $p(q_{[j]}|n_{[i]})$ is the conditional probability of flow rate $q_{[j]}$ given n rills, and $D_r(q_{[j]})$ is the detachment/deposition associated with flow rate $q_{[j]}$. Brackets on the subscripts i and j indicate discrete values for channel density and flow rate.

Deposition is also a function of channel shape. In the case of expected detachment/deposition on bare soil (Lewis et al.,1991), the channel shape is a function of flow rate; thus, Lewis et al. modeled channel shape with a deterministic relationship. In the case of grass filters, channel shape varies widely across a given segment for the same flow rate and is dependent on microrelief. In the model used for determining sediment trapping in grass filters, channel shape was also represented stochastically and sediment deposition/detachment was modeled as a function of flow rate as well as the channel shape, expressed as $D_r(q,W/D)$.

Equation II.3.4 can be modified to account for stochastic distribution of channel shape (W/D given q) associated with each flow rate. The modified equation used for determining the expected deposition in grass filters can be finally given in discretized form by

$$E(D_p) = \sum_{i=1}^{imax} p(n_{[i]})\, n_{[i]} \cdot \left[\sum_{j=1}^{jmax} p(q_{[j]} | n_{[i]}) \left[\sum_{k=1}^{kmax} p(W/D_{[k]} | q_{[j]})\ D_r(q_{[j]}, W/D_{[k]}) \right] \right] \quad \text{(II.3.5)}$$

where $p(W/D_{[k]} | q_{[j]})$ is the probability of W/D given flow rate q. The indexes i, j and k refer to the number of rills/channels, number of flow rates given n rills/channels, and the number of possible W/D values for a flow rate respectively.

Fundamental Methods

Parameters such as transport capacity, deposition, detachment, sediment load and particle size distribution are calculated using a physically based approach. Parameters are calculated for a given flow rate $q_{[j]}$ and its associated channel shape $W/D_{[k]}$.

Transport Capacity

Transport capacity is predicted using the calibrated version of the Einstein's equation (Tollner et al., 1982) specifically developed for grass filters,

$$\Psi = 1.08\,(\phi)^{-0.28} \quad \text{(II.3.6)}$$

where the Ψ is Einstein's shear intensity factor given by

$$\psi = (SG-1)\,\frac{d_{pd}}{S_g R_{sd}} \quad \text{(II.3.7)}$$

and Φ is the transport rate factor given by

$$\phi = \frac{q_{sd}}{\gamma_s \sqrt{(SG-1)\,g d_{pd}^{\,3}}} \quad \text{(II.3.8)}$$

where S_g is the ground slope, SG is the particle specific gravity, γ_s is the particle weight density in lbs/ft^3, d_{pd} is the representative particle diameter in mm, and R_{sd} is the spacing hydraulic radius in ft given by

$$R_{sd} = \frac{S_c d_f}{S_c + 2d_f} \quad \text{(II.3.9)}$$

where S_c is the grass media spacing and d_f is the depth of flow. For computational purposes the Einstein relationship can be rearranged as

$$q_{sd} = \frac{K(R_{sd}S_g)^{3.57}}{d_{pd}^{2.07}} \qquad \text{(II.3.10)}$$

where K is a constant given as

$$K = (1.08)^{3.57}\gamma_w g^{1/2} SG(SG-1)^{-3.07} \qquad \text{(II.3.11)}$$

In the above relationship R_{sd} is in ft, d_{pd} is the particle diameter in mm, γ_w is the density of water in lbs/ft^3, g is the acceleration due to gravity in ft/sec^2 and q_{sd} is the transport capacity in lbs/sec/ft width.

Equation II.3.10 can be used to calculate transport capacity for uniform particle sizes. For calculating the transport capacities for varying particle sizes in a sediment mixture, the approach by Hirschi (1985) was used to modify Einstein's equation. Hirschi (1985) used Yang's equation for determining the transport capacity. In his approach the transportable concentration corresponding to d_{50} was determined, and the potential concentrations of individual particle types were then estimated by assuming that the fraction of the transportable concentration filled by an individual particle type was the same as its fraction of the sum of the transport capacities of each type if alone in the flow. In our case, since Einstein's equation was used, d_{65} was the characteristic particle size used to determine transport capacities. The procedure is given as

- Calculate transport capacity using Einstein's equation for all types of particle sizes (particle types, i = 1 to 6) in the sediment mixture. Let transport capacity for any particle type be T_{ci}.
- Determine the sum of the transport capacities (ΣT_{ci}) and find the ratio of transport capacity of each particle type to the sum ($R_i = T_{ci}/\Sigma T_{ci}$).
- Determine transport capacity (T_{cs65}) corresponding to D_{65}.
- Determine the transport capacity for each particle size in the sediment mixture given as $T_i = R_i \times T_{cs65}$

Deposition

Deposition is modeled using the approach developed by Hayes et al. (1979) for sediment deposition (GRASFIL) in grass filter strips. As described earlier (see Chapter II.2 for details), GRASFIL simulated sediment deposition in grass filter strips by assuming shallow overland flow and by dividing the grass filter length into four component zones [(A(t), B(t), C(t) and D(t)] whose individual length was a function of time. Zones A(t) and B(t) are zones where sufficient deposition has occurred to form a sediment wedge. Zone C(t) is the zone where the deposited sediment is sufficient to cover the layer of grass litter on the bed, and thus initiate bed load transport. Zone D(t) represented the zone where the litter layer was still exposed and

sediment particles reaching the bed were assumed to be trapped. In other words zone D(t) did not have any bed load transport.

Deposition is assumed to occur when the sediment load exceeds the transport capacity. Two conditions are considered here, deposition of sediment when sufficient previous deposition has not occurred with bed load unavailable and deposition when bedload is available.

CASE 1: Deposition with no Significant Previous Deposition. This condition occurs when the depth of deposited sediment has not yet covered the grass debris, and thus all sediment reaching the floor is trapped. For such a condition Tollner et al. (1976) proposed the following equation for sediment trapping

$$T_s = \exp(-1.05 \times 10^{-3} R_e^{0.82} N_f^{-0.91}) \qquad \text{(II.3.12)}$$

where T_s is the trapping efficiency, R_e is the flow Reynolds number given by

$$R_e = \frac{V_m R_{sd}}{\nu} \qquad \text{(II.3.13)}$$

where V_m is the velocity of flow through the grass, ν is the viscosity of flowing water, and N_f is the fall number which is given by

$$N_f = \frac{V_s L_t}{V_m d_f} \qquad \text{(II.3.14)}$$

where V_s is the particle settling velocity for individual particle sizes, L_t is the length of the flow path through the filter, and d_f is the depth of flow through grass.

The above expression for trapping was developed by Hayes et al. (1979) for modeling sediment trapping considering the complete length of the filter. For a modeling approach in which the filter length is divided into segments and the total trapping for the filter determined by summing up the trapping efficiencies for individual segments, the expression needs to be modified. This modification was made by inclusion of a correction factor C_f.

In developing the correction factor, trapping is computed from a filter of length L_t, considering a similar filter with the same length but subdivided into 'n' segments as shown in Figure II.3.1. The trapping efficiency of both filters will be equal as they have the same total length and can be given by

$$q_i(1-TE_t) = q_i(1-TE_n)^n \qquad \text{(II.3.15)}$$

where q_i is the incoming sediment load, TE_t is the trapping efficiency for the full length of the filter and TE_n is the trapping efficiency for each of the n segments of equal length. Equation II.3.15 can also be expressed as

$$q_i\,[1-\exp(-AR_{en}^{b}N_{fn}^{c}C_f)]^n = q_i\,[1-\exp(-AR_{et}^{b}N_{ft}^{c})] \qquad \text{(II.3.16)}$$

where R_{et} and N_{ft} are the Reynold's and fall numbers for the full filter length, R_{en} and N_{fn} are the Reynold's and fall number for each of the n segments and A, b, c are the constants as described in equation II.3.12. Evaluating equation II.3.16 and substituting for N_{fn} (using expression II.3.14) the correction factor C_f was found to be

$$C_f = \frac{n^c}{m}\ln[1-(1-e^m)^{1/n}] \qquad \text{(II.3.17)}$$

where m is given by

$$m = [-AR_{et}^{b}N_{ft}^{c}] \qquad \text{(II.3.18)}$$

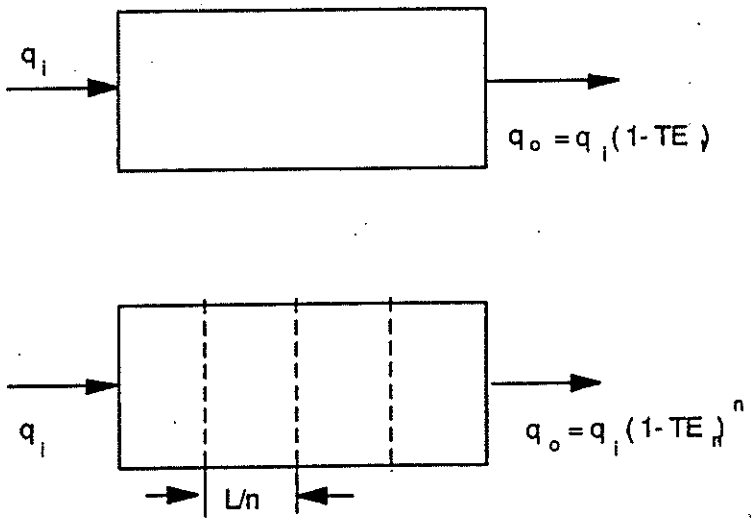

Figure II.3.1. Determining Trapping Efficiency of Discretized Filter Length.

Equation II.3.12 considers sediment trapping due to settling only, with deposition given by

$$D_p = q_s \cdot T_s \qquad \text{(II.3.19)}$$

where q_s is the incoming sediment load and T_s is the trapping efficiency defined earlier.

Sediment trapping is further increased due to infiltration. Hayes et al. (1984) evaluated the impact of infiltration on sediment load by assuming that the mass of sediment load in a given infiltration volume is either transported into the soil matrix by infiltration or is trapped on the surface. Infiltration in this case was modeled as the

difference between the flow coming into the filter and that exiting the filter. The infiltration rate i is given by

$$i = \frac{q_{wi} - q_{wo}}{L_t} \qquad \text{(II.3.20)}$$

where q_{wi} and q_{wo} are the inflow and outflow rates from the segment and L_t is the segment length. Hence, the total deposition considering infiltration was given by Hayes et al. (1984) as

$$D_p = q_s \left[\frac{T_s + 2I(1-T_s)}{1 + I(1-T_s)} \right] \qquad \text{(II.3.21)}$$

where I is the infiltration parameter defined by

$$I = \frac{q_{wi} - q_{wo}}{q_{wi} + q_{wo}} \qquad \text{(II.3.22)}$$

and other terms are as defined above.

CASE 2: Deposition with Sufficient Previous Deposition. When sufficient deposition has occurred and the grass debris is covered Hayes et al. (1982) observed that bed load transport is initiated. This sediment transport can be modeled using the calibrated version of the Einstein's bedload function (Tollner et al., 1982) which was discussed in the earlier section. With sediment transport available, the sediment deposited is given by (Hayes et al., 1985)

$$D_p = (q_{sd} - q_s) \cdot \frac{T_s + 2I(1-T_s)}{1 + I(1-T_s)} \qquad \text{(II.3.23)}$$

where the terms are as defined earlier.

The occurrence of either of the cases is determined by calculating the depth of sediment deposited in the channel and comparing it to the grass debris depth (see section on channel shape and sediment depth). In both cases the total deposition across the segment is divided by the segment length to give the deposition occurring per unit length of the filter.

Detachment

Detachment occurs when the sediment load in the flow is less than the transport capacity. Detachment is modeled using Foster and Lane's (1983) approach. Detachment in grass filter channels is modeled for three conditions.

CASE 1: Detachment of Parent Bed Material Before Reaching Non-Erodible Layer. This occurs when the shear of flowing water is greater than the critical tractive force of

the soil, and soil particles are dislodged from the bed, initiating bed scour. Detachment under such conditions is given as (Foster and Meyer, 1975)

$$D_r = D_{rc}\left(1 - \frac{q_s}{T_c}\right) \qquad \text{(II.3.24)}$$

where D_r is the actual detachment rate, D_{rc} is the maximum detachment rate, T_c is the transport capacity, and q_s is the sediment load. The maximum detachment rate D_{rc} is calculated using Foster and Lane's (1983) approach. Detachment is calculated as the difference between the shear stress acting along the boundary and the critical shear of the soil. The detachment rate is expressed by

$$D_{rc} = K_{ch}(\tau_s - \tau_c) \qquad \text{(II.3.25)}$$

where K_{ch} is the rill erosion coefficient. The shear distribution along the wetted perimeter is given by (Foster and Lane, 1983)

$$\tau_s = 1.35\bar{\tau}(1 - (1 - 2x_*)^{2.9}) \qquad \text{(II.3.26)}$$

where τ_s is the shear stress acting at point x, τ is the average shear stress given by γRS, and x_* is the normalized distance equal to the distance from the water surface to the point x along the wetted perimeter divided by the wetted perimeter. For case one, where channel depth has not reached the non-erodible layer, the maximum detachment rate D_{rc} is given by

$$D_{rc} = W\, K_{ch}(1.35\bar{\tau} - \tau_c) \qquad \text{(II.3.27)}$$

where W is the equilibrium width defined as a function of flow rate, Manning's roughness, slope, density, bulk density and critical tractive force by the Foster and Lane (1983) relationship. In this condition (before reaching the non erodible layer) the width attains a constant value for the parameters mentioned above and maintains this value until the rill depth is greater than the depth to non erodible layer. The Foster model (1982) computes equilibrium width through a number of steps. In this model, since the top width of the rill/channel is already defined, it is assumed that the top width is equal to the so called equilibrium width, that the channel maintains a constant shape, and that all points along the channel boundary move down at the same rate. Under such an assumption τ_s is equal to 1.35 τ at $x_* = 0.5$. Critical tractive force for soil under grass ($\tau_{c\,cov}$) is determined by increasing the critical shear stress for bare soil by a factor as used in CREAMS. Thus the factored value for critical tractive force can be given by

$$\tau_{c\,cov} = \frac{\tau_{soil}}{(n_{bov}/n_{cov})^{0.9}} \qquad \text{(II.3.28)}$$

where τ_{soil} is the critical shear for bare soil conditions, n_{bov} and n_{cov} is the Manning's roughness corresponding to bare soil and grass cover conditions respectively.

CASE 2: Detachment of Parent Bed Material After Reaching the Non-Erodible Layer. Detachment under this conditions occurs only on the side walls, since the channel is assumed to cease downward propagation but increases in width till it reaches the final equilibrium width. The maximum stress occurs at the channel wall and changes with time as flow depth decreases with increasing width. The maximum detachment rate is given as

$$D_{rc}=2K_{ch}(\tau-\tau_c)\,d_{ne} \qquad \text{(II.3.29)}$$

where d_{ne} is the depth to non-erodible layer, τ is the shear stress acting on the channel wall, determined using equation II.3.26 in which x_* is defined as

$$x_*=\frac{d_f}{W_f+2d_f} \qquad \text{(II.3.30)}$$

where W_f is the top width of the channel when it reaches the non erodible layer.

CASE 3: Detachment of Deposited Bed Material. Detachment in this case occurs on the delta formed due to prior deposition. Since it is assumed that only particles greater than 37 micron are deposited in the delta, the detachment is also restricted to particle sizes greater than 37 micron. The equation used for calculation of detachment is same as that used for Case 1. The critical shear required for detachment is determined using Shield's curve (1977).

Particle Size Distribution

Changes in particle size fractions due to deposition are determined. It is assumed that change in particle size due to infiltration is uniform across all particle sizes. The exiting fraction for a particle class is given as

$$f_{r_i}{}^{n+1}=f_{r_i}{}^{n}\cdot\frac{(1-TE_i)}{(1-\sum_{i=1}^{i=b}TE_i)} \qquad \text{(II.3.31)}$$

where f^n_{ri} is the incoming fraction for particle size i, f^{n+1}_{ri} is the exiting fraction for the particle size i, TE_i is the fraction trapped for the particle size i, and b is the number of particle sizes under consideration. For the coarser particle size range (Barfield, Warner and Haan, 1983) the new particle size distribution is developed under the assumption that only the larger particle sizes are trapped in the segment under consideration. Hence, for this model it was assumed that when the d_{50} for the distribution is greater than 37 micron, the particle size distribution shall be updated using the fraction trapped for particle sizes greater than d_{50}. For d_{50} values less than 37 micron the fraction trapped across all the particle sizes were considered for updating the distribution.

Changes in particle size distribution due to detachment are assumed not to occur. Change in particle size distribution is determined at the end of every segment.

Change in Channel Shape

Change in channel shape is computed after deposition or detachment of sediment. The change in channel depth is given by

$$\delta_{ch} = \frac{D_p}{W \rho_{soil}} \qquad \text{(II.3.32)}$$

where δ_{ch} is the change in channel depth, D_p is the deposition per unit length and ρ_{soil} is the bulk density of soil. The new depth after deposition/detachment is given by

$$d_{t+1} = d_t + \delta_{ch}\ \Delta t \qquad \text{(II.3.33)}$$

where d_{t+1} is the channel depth after deposition/detachment, d_t is the depth prior to the event and Δt is the length of the time period. Similarly, the depth of deposited sediment after time step Δt is given as

$$sedd^{t+\Delta t} = sedd^{t} + \delta_{ch} \qquad \text{(II.3.34)}$$

where $sedd^{t+\Delta t}$ is the depth of sediment after time Δt and $sedd^t$ is the sediment depth at time t.

Summary

A model is presented which could predict sediment trapping in grass filter strips considering channelization of flow. Since formation of rills/channels in the grass filter is a random process and virtually impossible to accurately predict deterministically for a given condition, it was decided to represent the process stochastically. Channel density, channel flow rates, and channel shapes were chosen as the parameters to be defined stochastically. Considering sediment continuity down the filter, an algorithm was developed which could determine the expected sediment deposition for a given filter length and distributions of channel density, flow rates and the channel shape.

Deposition/detachment in a single individual channel was modeled for six conditions using physically based fundamental methods. Transport capacities for the channels were determined using a calibrated version of Einstein's equation. Deposition in grass channels was modeled using an earlier developed approach by Hayes et al.(1979). Detachment was modeled using Foster and Lane's (1983) approach. Exiting particle size distribution was adjusted for deposition and detachment. Channel shapes changes with time were updated for deposition/detachment.

CHAPTER II.4

FIELD AND LABORATORY EXPERIMENTS

The objective of the field and laboratory experiments was to generate a database describing the behavior of grass filter strips as buffers and to use it to validate the model described in Chapter II.3. A description of most of the field laboratory experimental details was given in Part I of this report. This chapter describes the supplemental field measurements needed for this study and the laboratory procedures used to collect the data. This includes additional details on surface profiles and filter media density.

Experimental Design

The experimental setup consisted of six sets of plots, each consisting of an erosion plot and a filter strip located on moderate slopes. Runoff was directed through the variable length filter strips. Rainfall was generated on the erosion plots using a rainfall simulator.

Two types of erosion plots were utilized, conventional tillage and minimum tillage.

Surface Profile Measurements

Additional field measurements needed, besides those discussed in Part I, were surface profiles with the filter media. These values were used to develop flow networks.

Prior to and after each run, surface profile measurements were taken on the grass filter strips. This consisted of measuring relative elevations of the soil surface in the grass filter every six inches across the plot width and every foot along its length. This data was collected to determine preferential flow paths through the filter and to delineate the location of sediment deltas. Survey measurements were taken using an electronic total station instrument (TOPCON) and referenced to a stationary benchmark established for each filter.

Filter Media Density

Filter media density was also measured by counting the number of grass stems present in two six inch square samples on each filter strip. This was done to determine the average representative grass spacing in the filter. Dead detached stems, grass clippings and other debris were not accounted for.

CHAPTER II.5

DEVELOPMENT OF MODEL PARAMETERS

The parameters required for development of the validation and general model were derived from experimental observations made during the field study. The two types of parameters required were probabilistic parameters and parameters required for the deterministic approach used in computation of deposition/detachment of sediment.

Probabilistic Parameters

Probabilistic parameters to be developed included the number of channels, the probability associated with the number of channels, probability distribution of flow rates and probability distribution of width to depth, W/D, ratios for the channels. These parameters were developed based on the topographic measurements taken on the grass filter prior to and after each storm event during the field study.

Determination of Preferential Flow Paths/Channel Networks

Generation of Data Set. Preferential flow paths passing through the grass filter were determined using the grass filter microtopography data and a digital elevation DEM model (Storm et al., 1990). The program takes a grid of input raster elevations and predicts the flow network on the given surface. A detailed description of the model is given in Storm (et al., 1990). The grid of surface elevation values for the grass filter was generated through the steps summarized below.

Topographic measurements on the grass filter were taken at every six inches along the width and at every one foot along the length of the filter, as described in Chapter II.4. The input grid for the DEM model should be at equal distance intervals along both axes. Hence, a linear interpolation was done to generate elevations at every 1" intervals in both directions (x and y directions). Storm (et al., 1990) found that a random component was also needed in the interpolation to allow the DEM model to generate reasonable values. The equation used for the interpolation (for example for the y direction) is

$$z = z_o + (y - y_o)\,[\,(z_1 - z_o) / (y_1 - y_o)\,] + r\sigma \qquad \text{(II.5.1)}$$

where z_o and z_1 are the measured values of elevation at y_o and y_1 respectively, r is the random variable generated using a random surface generator and σ is the standard deviation of elevation.

After generation of the 1" grid, two rows of high numerical values were added at the top and the sides representing plot boundaries, thus forcing the DEM model to restrict the flow drainage within the area.

Generation of Flow Networks. The channel/rill networks were generated using the DEM model (Jenson and Dominque, 1988). The program considers a surface discretized into a grid of rectangular cells, with each cell having its own elevation value, and determines the flow path over the surface. The program also determines the fraction of the drainage area draining up to any particular point. Given the matrix of elevations, the program generates two matrices having the flow accumulation values and the flow directions for each of the cells. The accumulation value for each cell is the number of upstream cells draining into that particular cell. Flow directions for a cell are given from numbers one through eight representing the eight possible flow directions.

As defined above, the accumulation value for a cell represents the number of upslope cells draining into it. Hence, if uniform runoff is considered over each of the cells in the discretized plot, the accumulation value at a point will be a measure of the flow to that point. The DEM model provides accumulation values and the direction numbers for all the cells but does not delineate the rill network. The rill network is delineated by first defining the necessary condition for formation of a rill. A rill is formed when sufficient concentrated flow exists, which is represented in the DEM model by an accumulation value. Hence the rill can be supposed to exist when the accumulation value at a point exceeds a specified minimum value, which is equivalent to setting a minimum flow rate. This minimum accumulation value is called the "threshold value".

Limitations of the DEM Generated Flow Networks. Some limitations of the DEM model should be noted. The DEM model allows flow paths to converge to a single cell but does not allow flow paths to diverge from a single cell, i.e, bifurcation (splitting) of flow is not simulated. In actual field conditions partitioning of flow from a single flow path into two or more flow paths was observed. At present, there are no techniques available for generating bifurcation.

Flow Channels Due to Incoming Runoff and Rainfall. Incoming flow at the top of the filter was distributed along its width at ten inlet points. Flow paths generated as a result of surface runoff coming into the filter (hereby referred to as *runoff channels*) were manually traced using the spatial and volumetric inflow distributions at the top of the filter and the channel networks generated by DEM. An example of how runoff channels were delineated is shown in Figure II.5.1. Rills/channels developed at an intermediate point (having a accumulation value greater than the threshold) of the filter were not classified as runoff channels as no runoff flow existed in them.

Rainfall was assumed to be uniformly distributed across the full length of the filter. Hence accumulation values for each cell generated from the DEM corresponded to the runoff generated due to rainfall on the cell and accumulation values at a point were a measure of the flow occurring at that point (unlike the earlier case of incoming runoff). The network generated was the rill/channel network due to rainfall.

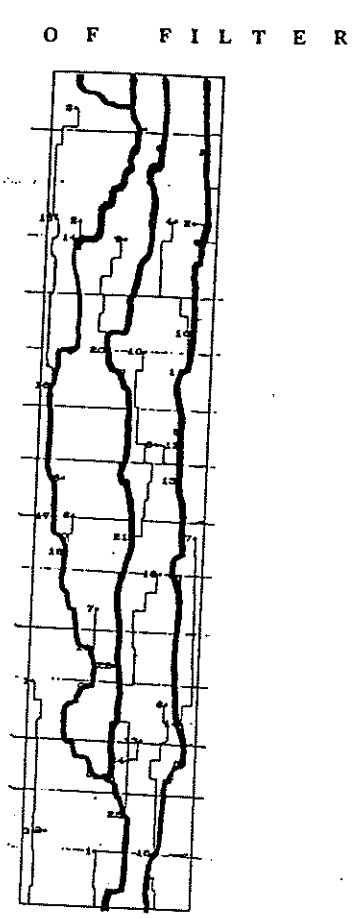

Figure II.5.1: Flow Paths Due to Incoming Runoff (thick lines) Superimposed on Channel Network Generated Due to DEM (represented by thin lines).

Probability Distribution for Channel Densities

Approaches for determining probability distributions for rainfall and runoff rills/channels were similar. Probabilities were determined for channel densities at every three feet along the filter length combining data from all the plots. Further probability values were also determined using fitted distributions to the data. The following steps were performed in determination of the probability distribution.

Channel Density and Probability Density Function. A plot of channel density along the filter length for all the grass filter plots is as shown in Figure II.5.2 and II.5.3. Deviation from the mean channel density was chosen as the statistic to be distributed. Deviation values at the selected cross sections from all the plots were then combined to develop the distribution.

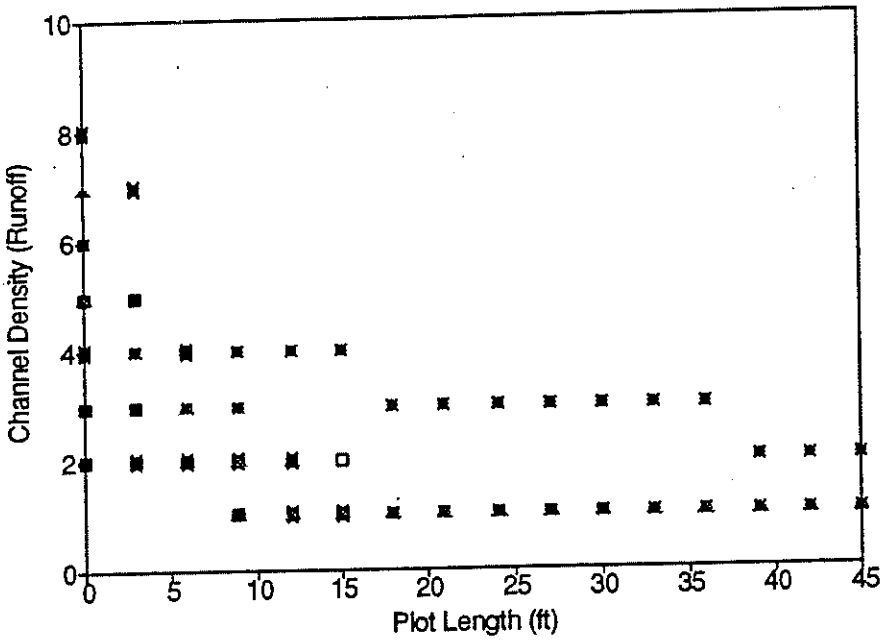

Figure II.5.2: Densities Along Filter Length for Runoff Channels.

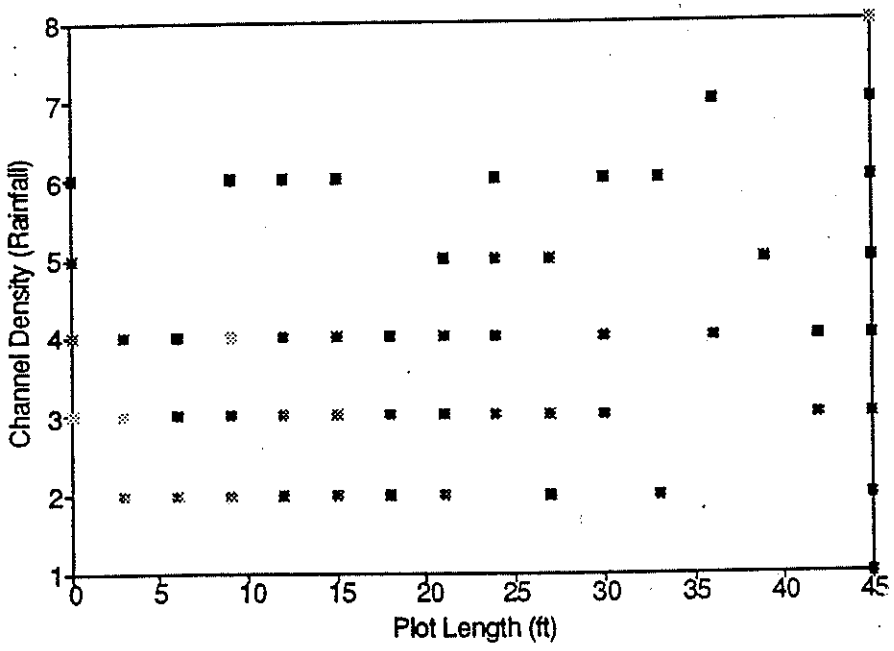

Figure II.5.3: Densities Along Filter Length for Rainfall Channels.

Since the data was discrete in nature, a Binomial distribution was fit to the data, following Lewis et al. (1991). The Binomial distribution is defined by

$$p(x) = \frac{T!}{x!\,(T-x)!} P^{x}(1-P)^{(T-x)} \quad if \quad x=0,1.....T \qquad \text{(II.5.2)}$$

$$0 \qquad otherwise$$

where x is the discrete value, p(x) is the probability corresponding to x, P is the probability parameter and T is the trial parameter. The Binomial distribution is non-negative in nature, thus the deviation values were made positive by adding the maximum observed value of each data point. Thereafter, binomial distribution parameters were then generated using UNIFIT, a statistical software package (Law and Vincent, 1983). Results are as shown in Table II.5.1. The actual distribution and the fitted Binomial Distribution are as shown in Figures II.5.4 and II.5.5.

Table II.5.1 Binomial Parameters for Channel Densities

Channel Density	Trial Parameter	Probability Parameter	Transformation Coeff.
Runoff	7	0.12842	+2
Rainfall	12	0.21927	+2

Probability Density Functions for Channel Flows

Probability density functions for runoff and rainfall flows were determined by fitting standard distributions to the accumulation data. The distribution of flow rates in the channels at any cross section was dependent on the total runoff at the cross section and the number of channels across the section. To avoid determining pdfs for each section the flows across the sections were normalized. The methodology for determining the pdf values was similar for both runoff and rainfall flows.

Flow in Runoff Channels. As defined earlier, runoff channels were those that carried runoff flow originating from the top of the filter. Sediment laden runoff naturally entering the filter strips from erosion plots was not uniformly distributed across the filter width. The variation was determined by measuring inflows at the ten inlet points on the sampler. Measured flows at each of these points was then normalized to the mean flow across the section to determine the normalized distribution of the flow.

At the topmost section, the flow from each inlet point was distributed to existing channels and the normalized flow in each of the channels determined. Similarly each of the channels were followed down the plot and the normalized flow values were determined by summing the flows from all contributing channels and

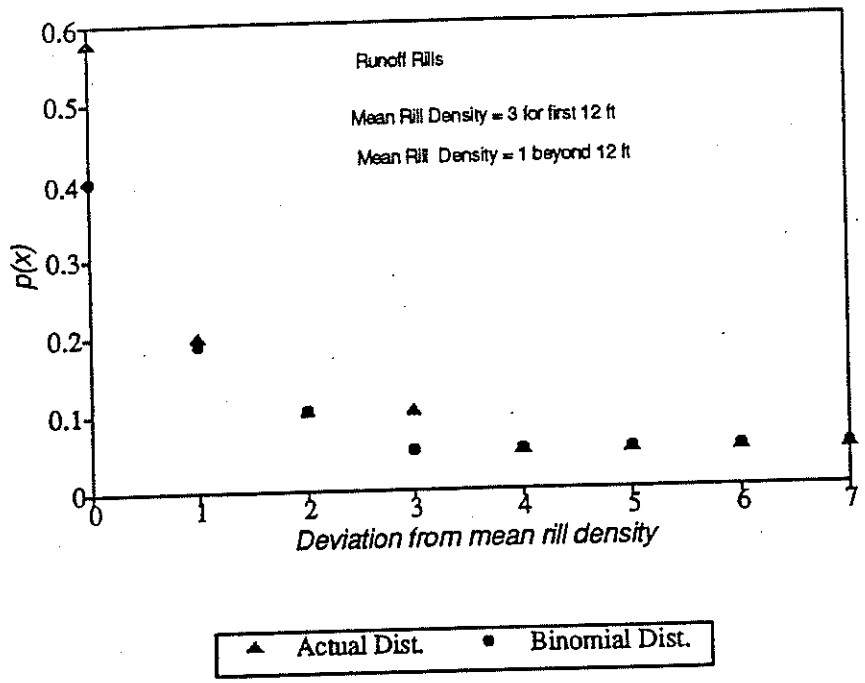

Figure II.5.4. Actual and Binomial Distribution for Runoff Channel Density.

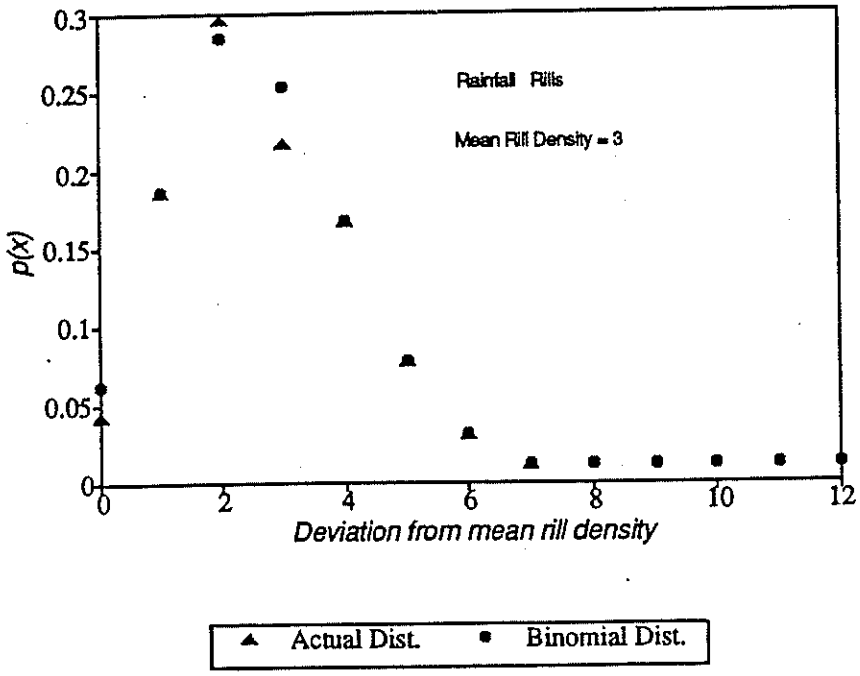

Figure II.5.5. Actual and Binomial Distribution for Rainfall Channel Density

subtracting infiltration. At each of the sections, flow values were normalized to the mean flow so that flow values could be independent of the total cross sectional runoff and the number of rills/channels at that section. With the given normalized value, the probability for the flow could be found for any combination of total cross sectional flow and number of channels. The normalized flow was determined by

$$q_n = \frac{q}{Q/n} \qquad \text{(II.5.3)}$$

where q_n is the normalized flow rate, q is the actual flow rate in the channel, Q is the total runoff across the specified cross section and n is the number of rills. Normalized flow values were determined at cross sections every three feet down the plot.

Flow in Rainfall Channels. Flow in channels due to rainfall on the filter was determined from accumulation values for the cell at that point. As described earlier these channels were assumed to be formed when the accumulation value exceeded a threshold limit. Hence normalized flow due to rainfall in each of the channel was equal to the ratio of the accumulation value for that channel at the section to the mean accumulation value at the section. The underlying assumption to this procedure is that the rainfall is generated uniformly across the plot. Similar to the runoff flow, normalized rainfall flow values were determined for each channel at points every three feet down the plot.

Probability Distribution for Runoff and Rainfall Flows from Data. The procedure for determining the probability values for rainfall (generated on the filter) and runoff flows is similar. As discussed in the Chapter II.3 on Model Development, flow rate distribution is dependent on the channel density. Hence flow data for both runoff and rainfall flows was grouped into two data sets each. The first data set had normalized flows for a channel density less than or equal to three across the section. The second data set was for flows with channel density greater than three. Each data set was a sum of all the normalized flow values for all the filter plots. As normalized flow rate is a continuous value, histograms were developed using suitable flow rate increments, shown in Figure II.5.6 through II.5.9.

Since flow rate is a continuous variable, a continuous distribution like Gamma was chosen following Lewis et al. (1991). Lewis et al. had shown that Weibull and Gamma distribution provided the best fit to flow rate distributions observed in the rills. Assuming this was true in our case also, Weibull and Gamma distribution were selected for consideration. Finally the Gamma distribution was chosen because it provided a methodology for determining the pdf for the sum of two independent distributions (rainfall and runoff flows). The Gamma distribution is given by

$$f(x) = \begin{cases} \dfrac{(x-\gamma)^{\alpha-1}\exp[-(x-\gamma)/\beta]}{\beta^{\alpha}\Gamma(\alpha)} & \text{if } x > \gamma \\ 0 & \text{otherwise} \end{cases} \qquad \text{(II.5.4)}$$

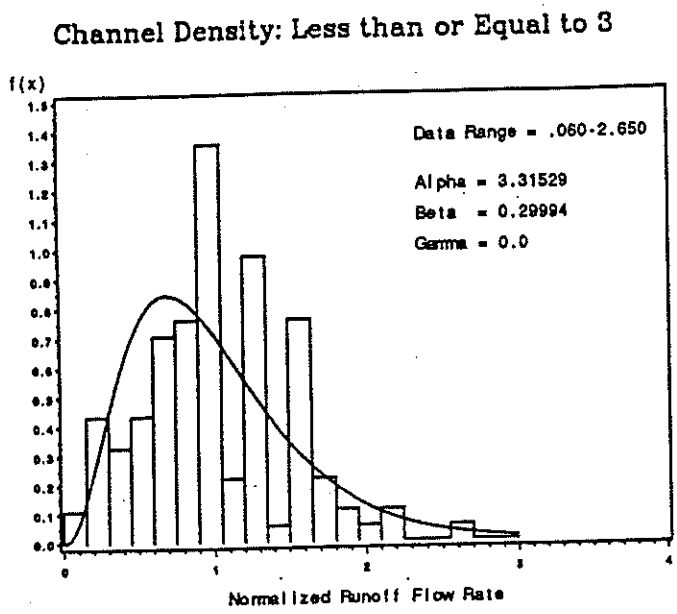

Figure II.5.6. Data and Fitted Runoff Flow Rate Distributions.

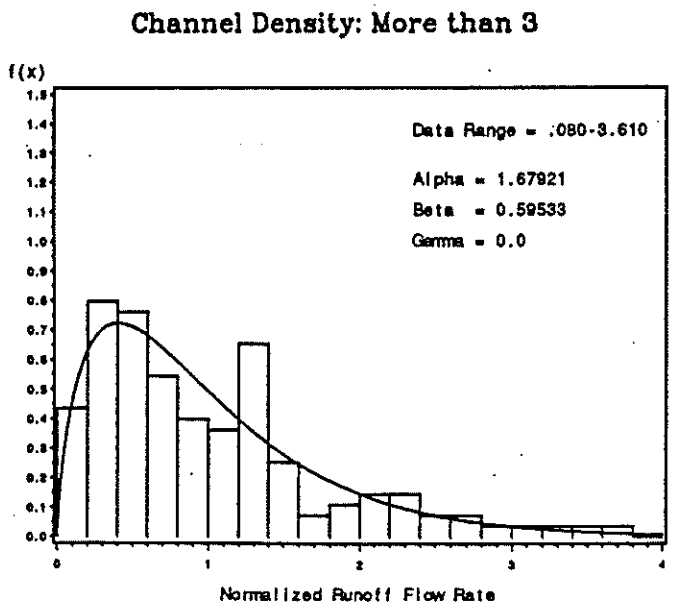

Figure II.5.7. Data and Fitted Runoff Flow Rate Distributions.

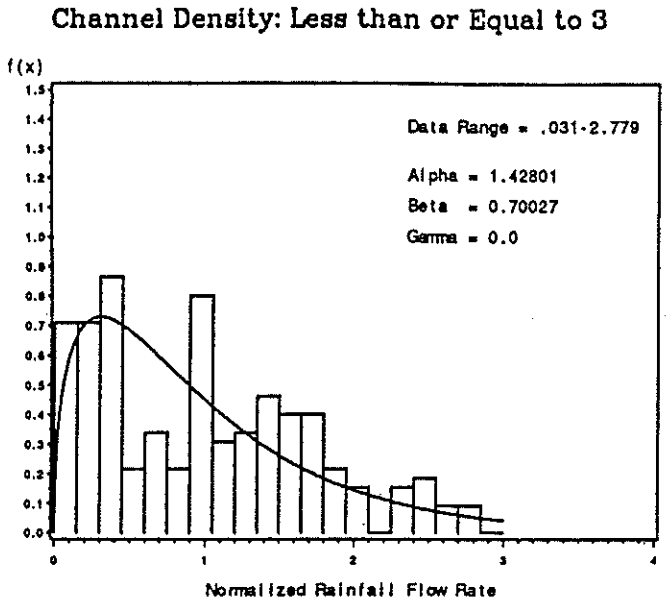

Figure II.5.8. Data and Fitted Rainfall Flow Rate Distributions.

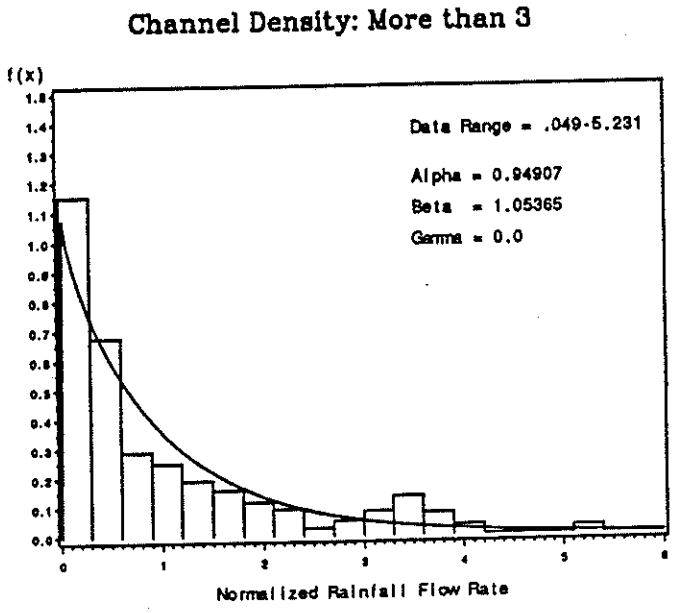

Figure II.5.9. Data and Fitted Rainfall Flow Rate Distributions.

where α is the shape parameter, β the scale parameter γ is the location parameter, and $\Gamma(\alpha)$ is the gamma function, defined by

$$\Gamma(z) = \int_0^\infty t^{z-1}e^{-t}dt \quad \text{for any real number } z > 0 \qquad \text{(II.5.5)}$$

The equation used in the program was the cumulative probability equatión which is given by

$$F(x) = \begin{cases} 1-\exp[-(x-\gamma)/\beta] \sum_{j=0}^{\alpha-1} [(x-\gamma)/\beta]^j/j! & \text{if } x > \gamma \\ 0 & \text{otherwise} \end{cases} \qquad \text{(II.5.6)}$$

where F(x) is the cumulative probability associated with x and other parameters are as explained above.

Gamma distributions were generated for both data sets determined above using UNIFIT. The parameters α and β were estimated with the assumption that γ is zero using the method of maximum likelihood. The estimated parameters are given in Table II.5.2 and the fitted distributions using UNIFIT software are shown in Figures II.5.6 through II.5.9. As can be seen from the figures, distributions become skewed to the left as the channel density across a section increases, indicating a larger number of smaller flows (as the total runoff is spread across more number of rills/channels).

Probability for W/D Ratios

Channel shape was observed to vary across the filter width for the same flow rate, requiring a stochastic representation. Cross sections for channels were determined at points every three feet down the filter. Since there was no distinct difference between channel shapes prior to and after deposition of sediment no differentiation was made.

Determination of W/D, Area and Perimeter Values. Cross sectional elevations for channels at the selected sections every three feet down the filter were determined using the microtopography data. A typical cross section of a channel is as shown in Figure II.5.10. For each such channel, top width to depth ratios, wetted perimeter and cross sectional areas were determined for increasing depth values.

Flow Rate versus W/D ratios. Channel flow rates were determined for each W/D value using the corresponding area and hydraulic radius values and assuming a Manning's roughness of 0.1. A Manning's n of 0.1 was estimated based on literature values for flow through grass. These flow rates were then plotted versus their corresponding W/D ratios (as shown in Figure II.5.11) and a regression relationship between flow rate and W/D developed.

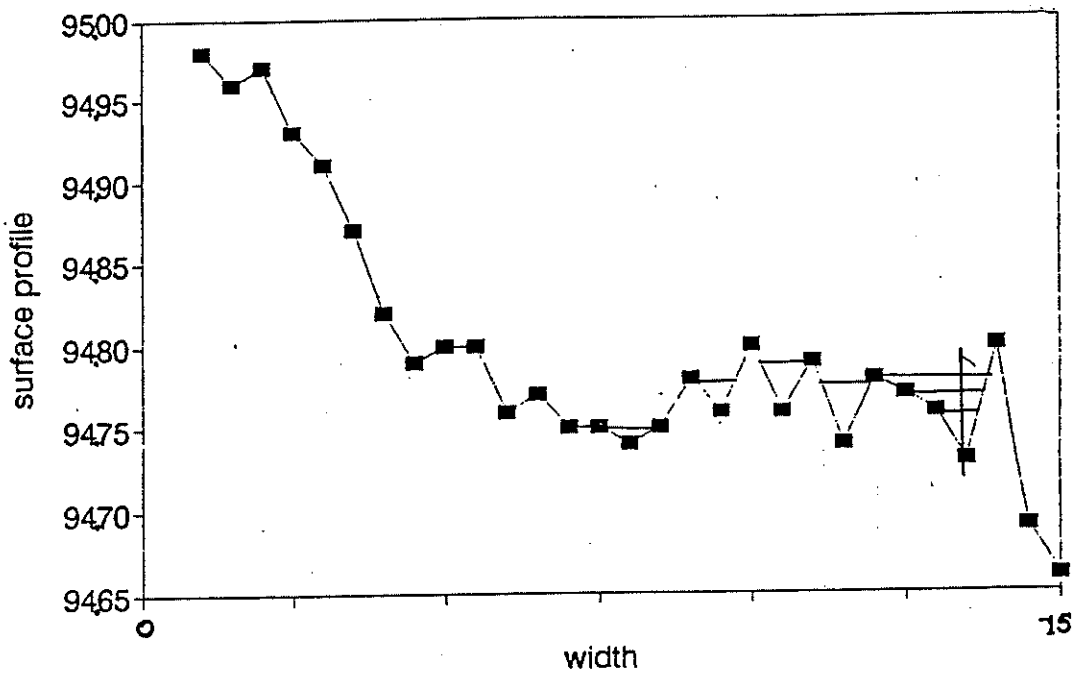

Figure II.5.10. Illustration of a Sample Cross Section of the Plot Used for Determination of W/D Ratios (units for width and depth are in feet).

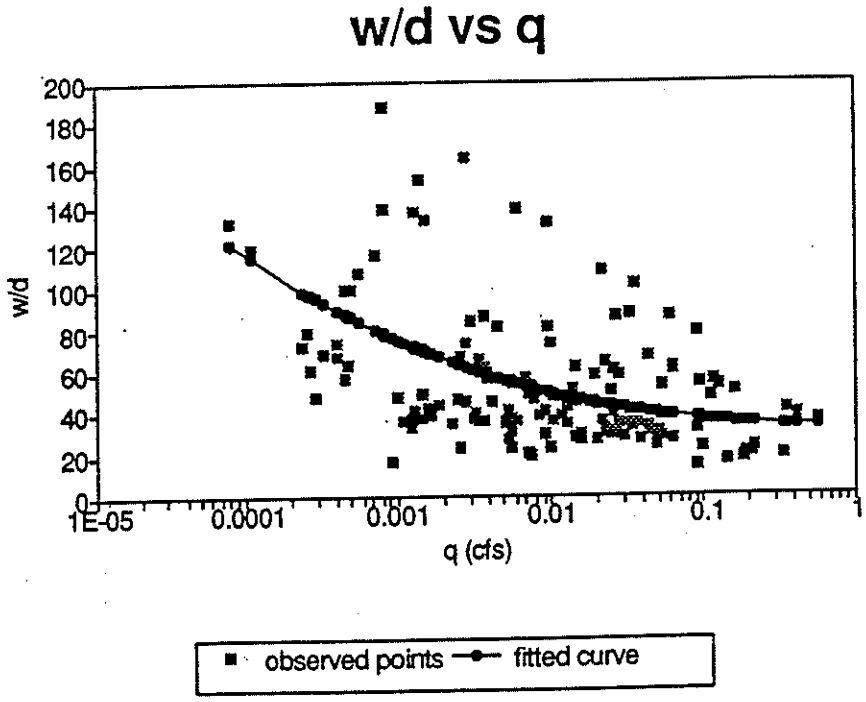

Figure II.5.11. Distribution of W/D with Flow Rate Showing Regression Relationship and Actual Data.

Probability Distribution for Normalized W/D data. W/D values for all the channels across all the plots were then grouped into data sets depending on their flow rates. Four data sets were generated corresponding to flows: (1) less than 0.001 cfs, (2) 0.001 to 0.01 cfs, (3) 0.01 to 0.1 cfs, and (4) greater than 0.1 cfs. W/D values were then normalized to the mean W/D value in the respective flow data group. This classification by flow rate was done so that a distribution of possible channel shapes could then be generated for any given flow rate and so that the normalized W/D distribution would be independent of the earlier assumed Manning's roughness values.

Table II.5.2. Gamma Distribution Parameters for Flow Rates

Condition		Shape Parameter α	Scale Parameter β	Location Parameter γ
I) Runoff Flows				
Less than channels	3	3.3152	0.2994	0.0
More than channels	3	1.67921	0.59533	0.0
II) Rainfall Flows				
Less than channels	3	1.42801	0.70027	0.0
More than channels	3	0.94907	1.05365	0.0

Fitted Distribution for Normalized W/D values. Since the normalized W/D values were continuous in nature, Gamma distribution was fitted to the data using the UNIFIT package. The estimated parameters are as given in Table II.3.4 and the fitted distributions are as shown in Figure II.5.12 through II.5.15.

Table II.5.3 Gamma Distribution Parameters for Normalized W/D Values

Flow Rate Condition q(cfs)	Shape Parameter α	Scale Parameter β	Location Parameter γ
1) $q \leq 0.001$	4.51927	0.21903	0.0
2) $0.001 < q \leq 0.01$	3.63776	0.26495	0.0
3) $0.01 < q \leq 0.1$	5.53387	0.19529	0.0
4) $0.1 < q \leq 1.0$	5.10372	0.18611	0.0

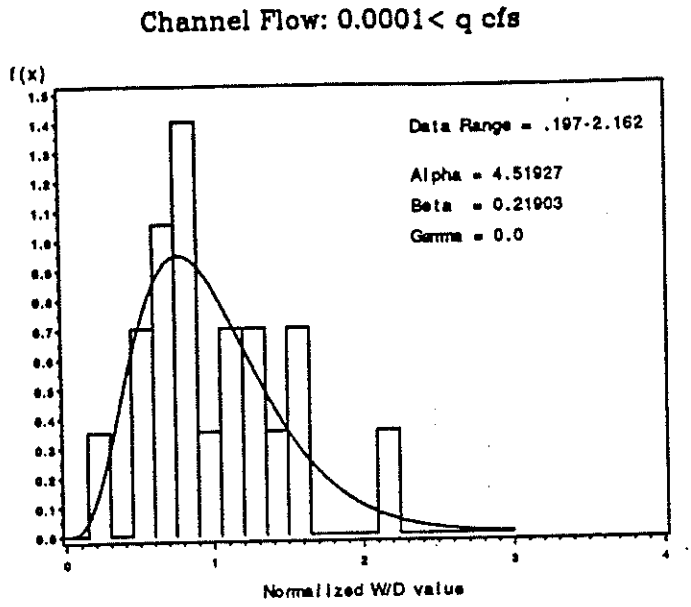

Figure II.5.12. Data and Fitted Gamma Distributions for Normalized W/D Data.

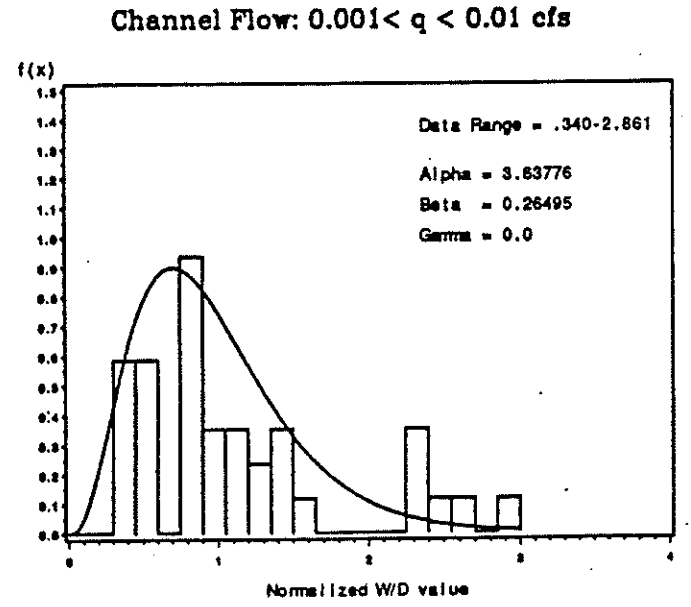

Figure II.5.13. Data and Fitted Gamma Distributions for Normalized W/D Data.

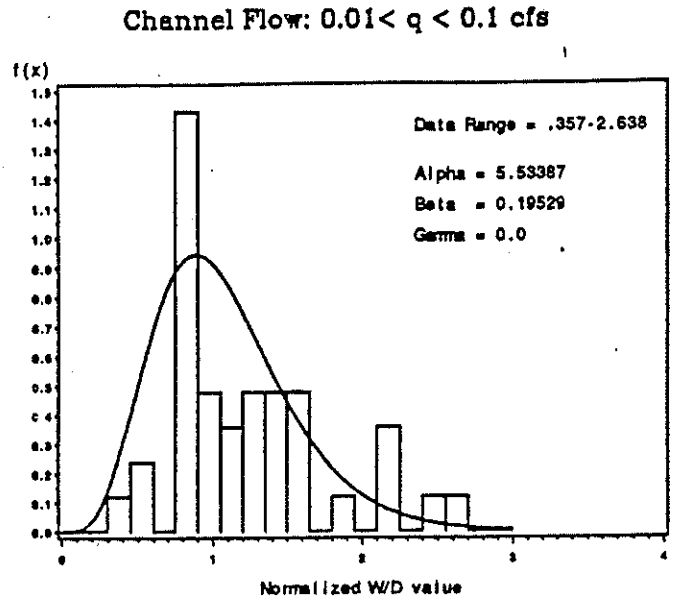

Figure II.5.14. Data and Fitted Gamma Distributions for Normalized W/D Data.

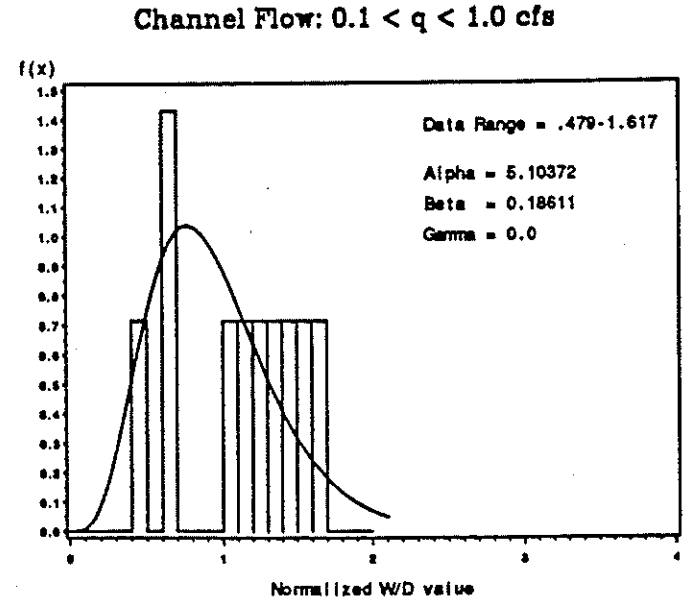

Figure II.5.15. Data and Fitted Gamma Distributions for Normalized W/D Data.

Model Parameters

Parameters used in the physically based fundamental methods were determined or estimated from experimental analysis and from the literature.

Hydrologic

Hydrologic parameters for the model were the incoming runoff hydrograph and sedigraph for the storm event runs and the runoff hydrograph generated due to rainfall. The inflow runoff hydrograph shows greater variation than the outflow. This variation likely included experimental error due to short measuring time for the inflow samples. For this reason the variation was filtered before input into the program using a 1:3:5:3:1 filter program.

Since infiltration rate on the filter was not measured, it was assumed that the incoming runoff rate would linearly decrease down the plot, i.e, infiltration was constant over the plot. Accordingly, the total incoming runoff rate at any segment between the top and the bottom of the filter was found by linear interpolation. Similarly, as the rainfall was assumed to be uniformly distributed, the runoff at any segment due to rainfall was proportional to the area draining up to that segment. For runoff generated due to rainfall a certain percent was assumed to have been infiltrated. This percent infiltrated was decided based on the percent infiltration observed for the runoff flows.

Sediment Load and Particle Size Distribution

Sediment concentrations in the incoming and exiting flows and their particle size distributions were determined through laboratory analysis. The incoming sediment flow rate was computed and input into the model. Smoothing was complicated using the same 1:3:5:3:1 filter program earlier used for flow filtering. Three particle size distribution curves were determined for each run wherever possible (depending on availability of sufficient sediment for tests) so as to define changes in sediment size with time. Hence three sediment size distributions were input for each model run. The particle sizes input into the model were selected such that a complete representation of the incoming sediment and the exiting sediment could be achieved. The particle sizes used are in the model were 2,000, 125, 63, 10 and 5 microns.

Manning's Roughness 'n'

The initial estimate of Manning's 'n' was 0.350. This value was based on literature data for flow through dense turf grass (Barfield, Warner and Haan. 1983). The other values selected for consideration were 0.20, 0.30 and 0.40. Lower values of Manning's n (0.2 and 0.3) were also considered to account for the possibility that roughness values may be less for channelized flow in the filters.

The values chosen were larger than those measured by Hayes et al. (1979) for laboratory studies (Manning's n around 0.012) of flow through artificial grass media.

These Hayes et al. (1979) values were for flow with depths of the order of 0.05 to 0.10 meters whereas the flows for this study were typically of the order of 0.002 m.

Critical Tractive Force

The critical tractive force values selected for the model was 3.2 N/m^2 for bare soil. An equivalent value under grassed conditions was determined using CREAMS methodology. The value for bare soil was taken from an earlier study done in similar soils (Storm et al., 1991). The accuracy of this value was not critical as field observations showed that detachment of parent bed material did not occur under grassed conditions, as the flow shear was much less than the critical tractive force.

Grass Spacing

Grass spacing at the experimental filter plots was measured and found to be 0.0127 m, which was found to be close enough to earlier reported values of 0.017-0.020 in the literature (Hayes et al., 1979).

Debris Depth

Debris depth as defined earlier is the amount of deposition required such that deposited sediment completely covers the grass debris and bed load transport is initiated. Measurement of this parameter was not included in the scope of this project hence an estimate had to be made. Based on visual observation the debris depth was estimated to be 0.012 m.

Depth to Nonerodible Layer and Bulk Density

Depth to non erodible layer and bulk density was estimated based on measurements made in an earlier study by Lewis et al. (1991) on soil erosion on similar soils. The depth to nonerodible layer was assumed to be 16.0 cm. A bulk density of 1090 kg/m^3 was used in the analysis based on the data from Storm et al. (1991). This value was for tilled soil.

Summary

Model computations required development of stochastic parameters and parameters used in physically based fundamental methods. Stochastic distributions were developed for channel density, channel flow rate and channel shapes as reflected by W/D values. Probability density functions were generated by fitting standard distributions to the data. A discrete binomial distribution was used for channel density and a Gamma distribution was used for flow rate and W/D data, parameters which are continuous in nature.

Parameters used for physically based methods were the runoff generated off the erosion plot, runoff generated on the filter strip due to rainfall, sediment load values for each time step and their accompanying particle size distributions. Also

input were Manning's roughness values for grass, critical tractive force, grass media spacing, debris depth and the depth to non erodible layer. Some of these parameters were generated from experimental observations and others estimated based on available literature values.

CHAPTER II.6

MODEL FRAME WORK

Based on the stochastic and physically based methodology developed in Chapter II.3 a sediment trapping model was developed to determine sediment trapping in riparian grass filter strips. Two models were developed based on the same physically based approach. The modeling approach was validated based on results obtained from the experimental filter strips using the validation model. In the validation model empirical probability values developed from data were used as input, as opposed to using fitted distributions to data, as discussed in Chapter 5. The effort in the validation model was to predict the actual trapping efficiency for individual plots as observed on the field.

The "general model" was developed so that it could be applied to generic filter strips under design conditions to do a sensitivity analysis. Furthermore, the general model also included effects such as the rainfall on the filter, which were not simulated in the validation model. Fitted distributions to channel density and flow rate data were used in the general model so as to increase the scope of applicability.

To determine the expected trapping, and account for the variability in parameters along the flow paths, the filter plots were discretized into segments along the filter length, and the storm event was discretized into suitable time steps. It was assumed that the parameters were uniform along the full length of a given segment. Using the discretized segments, the sediment continuity equation was solved down the length of the filter. Sediment load exiting a segment was the input load into the immediate downslope segment.

The Validation Model: Computational Framework

The aim of the validation model was to predict as accurately as possible the sediment trapping efficiencies for grass filters evaluated during experimental studies. As discussed in Chapter II.3, modeling was done using stochastic as well as physically based fundamental approaches. The stochastic variables input in the model were the channel density, channel flow rates, and the channel shapes (W/D values). For the validation case actual distributions were input for each of the parameters so as to closely simulate the actual situation observed during experimental studies for each of the filter plots.

Stochastic Variables

For the validation model the channel density (number of channels) formed as a result of incoming runoff was determined at every segment. The probability corresponding to that number was set as 1.0. The actual distribution of runoff flows derived from data were used at every segment corresponding to the respective channel density. Similarly, actual distributions for normalized variables

$(\frac{q}{Q/n}, \frac{W/D}{\overline{W/D}} \mid q, n)$ derived from data were also used. Procedures for development of these parameters are given in Chapter II.5.

Sediment Routing

As discussed earlier, computations are based on the assumption of sediment continuity along the segments of the filter. Since trapping was evaluated for each segment, sediment load at the middle of each segment for each flow rate was determined based on the incoming sediment load and approximated value of the exiting load. The average sediment load was determined by

$$q^n_{smid[j]} = (q^n_{s[j]} \cdot \theta) + (q^n_{so[j]} \cdot (1-\theta)) \qquad \text{(II.6.1)}$$

where $q_{smid\,[j]}{}^n$ is the sediment load at the middle of the nth segment for flow rate j, $q_{s[j]}{}^n$ is the sediment load coming into the nth segment, $q_{so[j]}{}^n$ is the exiting sediment load from the nth segment and θ is a coefficient having a value of 0.5.

Following Lewis et al. (1991) sediment load in each channel flow was proportioned according to the ratio of flow in the channel to the total flow across the segment, or

$$q_{s[j]} = \frac{q_{[j]}}{Q^n} \cdot Q_s{}^n = K_r \cdot q_{[j]} \qquad \text{(II.6.2)}$$

where $q_{s[j]}$ (kg/s) is the sediment load in the channel, $q_{[j]}$ (m^3/s) is the channel flow, Q^n (m^3/s) is the total flow across the section, $Q_s{}^n$ (kg/s) is the total sediment load entering the segment n and [j] indicates the discrete nature of flow rate. The ratio of $Q_s{}^n$ and Q^n is denoted as K_r or the partitioning coefficient in the model and is determined for every segment down the filter. Further details are given in Inamdar (1993).

Transport capacity

Transport capacity was calculated using Einstein's calibrated equation (equation II.3.6 in Chapter II.3). Transport capacity is determined for each particle class in the mixture, relative to the D_{65} of the sediment as explained in Chapter II.3. The D_{65} value is computed for each segment as the sediment size distribution changes down the plot. The particle sizes under consideration were divided into two particle classes - coarser and finer. Particle sizes greater than or equal to 0.037 mm were defined as coarse and smaller than 0.037 mm as fine. Hayes et al.(1979) proposed that only particles greater than or equal to 0.037 mm in diameter are trapped in the sediment wedge. Based on this assumption excess transport capacities for finer classes were neglected by equating their transport to the available sediment load in their respective class. This modification helped computationally to determine the trapping of finer sediment due to infiltration.

The hydraulic radius term used in equation II.3.9 in the computation of the transport capacity is the spacing hydraulic radius for the grass media.

Deposition/Detachment

Deposition/detachment is determined for every flow rate and its respective channel shape (represented by normalized W/D values). Total deposition/detachment is expressed in the model as the sum of deposition/detachment across all sediment sizes and is determined per unit length of the filter. Deposition/detachment in channels is modeled with six approaches listed below. Refer to Chapter II.3 for background details.

- *Case 1: Detachment of parent bed material before reaching the non-erodible layer.* Detachment in this case is given as

$$D_{r[j,k]}=D_{rc[j,k]}\cdot\left(1-\frac{q_{s[j]}}{T_{c[j,k]}}\right) \qquad \text{(II.6.3)}$$

  where $D_{r[j,k]}$ is the actual detachment rate (kg/s/m), $D_{rc[j,k]}$ is the maximum detachment rate (kg/s/m), $T_{c[j,k]}$ (kg/s) is the transport capacity and $q_{s[j]}$ (kg/s) is the sediment load corresponding to flow rate $q_{[j]}$ and is assumed constant over the range of channel shapes. Here [j,k] denotes the fact that the parameters are being determined for each flow rate and its respective channel shapes. $D_{rc[j,k]}$ is determined considering critical tractive force for covered soil and is given by equation II.3.25.

- *Case 2: Detachment of parent bed material after reaching the nonerodible layer.* Detachment in this condition occurs along the channel walls and is again determined by the above equation, but $D_{rc[j,k]}$ in this case is the detachment rate for a widening channel and is as given in equation II.3.29.

- *Case 3: Detachment of deposited material.* This detachment will mostly occur on the sediment deltas formed at the upslope end of the filter, hence detachment will be restricted to particle sizes greater than 0.037 mm. Detachment is given by equation II.6.3, and $D_{rc[j,k]}$ is determined using equation II.3.25 where the critical tractive force is determined using equation developed by Shulits and Hills (1968) based on the correction to Shield's curve (Gessler, 1971). In the original form the equations are given as

$$\tau_c=0.0215\ D_s^{0.25} \qquad for\ \ 0.0003< D_s <0.0009ft \qquad \text{(II.6.4)}$$

$$\tau_c=0.315\ D_s^{0.633} \qquad for\ \ 0.0009< D_s <0.0018ft \qquad \text{(II.6.5)}$$

$$\tau_c = 16.8\ D_s^{1.262} \qquad for\ \ 0.0018 < D_s < 0.022ft \tag{II.6.6}$$

$$\tau_c = 6.18\ D_s \qquad for\ \ D_s > 0.022ft \tag{II.6.7}$$

where τ_c is the critical shear stress (lb/ft^2) and D_s is the diameter in ft. The above equations are based on the assumption that $\gamma = 62.4\ lb/ft^3$, $\gamma_s/\gamma = 2.65$ and $\nu = 1.04 \times 10^{-5}$. In this model being developed critical tractive force derived from this equations is converted into N/m^2 before further computations.

- *Case 4: Deposition prior to the layer of grass debris being covered by sediment.* Deposition is modeled using equation II.3.21. The equation for a given flow rate and shape can be given as

$$D_{p[j,k]} = q_{s[j]}\left[\frac{T_{s[j,k]} + 2I(1 - T_{s[j,k]})}{1 + I(1 - T_{s[j,k]})}\right] \tag{II.6.8}$$

where $D_{p[j,k]}$ is the deposition in kg/s/m for a given flow rate and channel shape, $q_{s[j]}$ is the sediment load in the flow (kg/s), I is the infiltration parameter and $T_{s[j,k]}$ is the trapping efficiency. The definition of the terms is as given in Chapter II.3.

- *Case 5: Deposition after sufficient previous deposition has occurred such that bed load transport exists.* Deposition in such a condition is given as

$$D_{p[j,k]} = (q_{sd[j,k]} - q_{s[j]})\left[\frac{T_{s[j,k]} + 2I(1 - T_{s[j,k]})}{1 + I(1 - T_{s[j,k]})}\right] \tag{II.6.9}$$

where $q_{sd[j,k]}$ is the transport capacity, and the other terms are defined in Chapter II.2.

- *Case 6: No deposition/detachment when transport capacity equals the sediment load.*

Channel Shape

Before start of the storm event, channels are already existing in the filter. Channel shapes as defined by widths and depths, are not known. But since in this analysis channel shape must be defined before computations are made, a procedure was developed to determine tne probable initial channel widths and depths. Since we are considering a 15 foot wide filter it is known that the sum of the widths of all the probable channels (occurring in the filter) is limited to this filter width. Hence, if the W/D ratio for a channel was known, the width for the channel can be determined

using a initial trial value of depth and the W/D ratio. Using the same depth, widths of channels across all flow rates can be determined, thus determining the total width of the filter occupied by the channels. According to the assumption made earlier, this width should be equal to the filter width. If the occupied width is less than the filter width the initial assumed value of depth is incremented and the procedure repeated iteratively till the required result is achieved.

W/D ratios for the probable channels in the filter were defined by a range of W/D values. The range of W/D values for a channel was fixed considering the flow expected in the channel. For example the range of expected W/D values for a channel having a flow rate less than 0.001 cfs was between 30 to 200 (see Figure II.5.11).

Similarly ranges were also fixed for other flow rates. Channel depths at start of the storm event are determined utilizing the W/D values and their distributions. Depths of all the channels across the section are determined such that the sum of their widths does not exceed the plot width of 4.572 m. The computational procedure used is listed below.

- Initially a small value of channel depth 'd'(m) is assumed.

- Using the assumed channel depth and given a flow rate the probable sum of the channel widths across all the possible flow rates is determined and is given as

$$SW_{[i]} = \sum_{j=1}^{jmax} p(q_{[j]}|n_{[i]})\ possw_{[j]} \qquad \text{(II.6.10)}$$

  where $SW_{[i]}$ is the probable sum of the widths, $p(q_{[j]}|n_{[i]})$ is the probability of flow rate q given n rills/channels and $possw_{[j]}$ is the probable width corresponding to the flow rate $q_{[j]}$. The probable width is determined using the assumed depth d and the probable value of W/D for the flow rate.

- $SW_{[i]}$ determined above is for a single channel, to be applicable for the channel density across the section. $SW_{[i]}$'s for all channels are summed to get the total width at cross section occupied by the channels. If this total sum is less than the plot width the channel depth d (assumed in the first step) is increased and the computations repeated iteratively until the total sum is nearly equal to or less than the plot width of 4.572m . The probable sum of the $SW_{[i]}$'s is given as

$$TSW_i = \sum_{i=1}^{imax} n_{[i]} p(n_{[i]}) SW_{[i]} \qquad \text{(II.6.11)}$$

  where $TSW_{[i]}$ is the sum of $SW_{[i]}$'s for all channels, $p(n_{[i]})$ is the probability associated with $n_{[i]}$ number of channels.

- The final value of depth d which satisfies the above condition will correspond to the maximum W/D ratio for a given channel flow; hence, channel depths for other W/D ratios can be determined by simple proportionality.

After the first time step, the channel shape, which is approximated by a rectangular shape, will be updated as per the deposition/detachment condition. In case of deposition the channel depth will decrease, with width remaining unchanged. In detachment Case 1, the channel will increase in depth with width remaining constant or

$$d_{[j,k]}^{t+\Delta t} = d_{[j,k]}^{t} + m_{ch[j,k]} \Delta t \qquad \text{(II.6.12)}$$

where $d^{(t)}_{[j,k]}$ (m) is the channel depth at time t, $d^{(t+\Delta t)}_{[j,k]}$ (m) is the channel depth after time $(t + \Delta t)$ and m_{ch} is the rate at which the channel moves downward. In detachment Case 2, the channel depth will remain constant (as it reaches a nonerodible layer) and the channel width will increase. The increase in the width is for every flow rate and its channel shape and can be written as

$$W^{t+\Delta t}_{[j,k]} = W^{t}_{[j,k]} + \Delta W_{[j,k]} . \Delta t \qquad \text{(II.6.13)}$$

where $W^{t+\Delta t}_{[j,k]}$ (m) is the channel width after time Δt, $W^{t}_{[j,k]}$ (m) is the width at time t and $\Delta W_{[j,k]}$ is the change in width per unit time which is given as

$$\Delta W_{[j,k]} = \frac{D_{r[j,k]}}{\rho_{soil} d_{ne}} \qquad \text{(II.6.14)}$$

where $D_{r[j,k]}$ is the detachment rate, d_{ne} (m) is the depth to non-erodible layer and ρ_{soil} (kg/m^3) is the bulk density of the soil.

Exiting Sediment Flow and Particle Size Distribution

The exiting sediment flow is determined as the algebraic sum of the incoming sediment load and the expected deposition/detachment. The expected deposition or detachment, $E(D_p)$, (kg/s/m) is calculated by summation of the deposition or detachment across all the flow rates and their respective channel shapes as given by equation II.3.5. The exiting sediment flow is given as

$$Q_{so} = Q_s + E(D_p) . \Delta L \qquad \text{(II.6.15)}$$

where Q_s (kg/s) is the incoming sediment flow into the segment, Q_{so} (kg/s) is the exiting sediment flow, $E(D_p)$ is the expected deposition or detachment per unit length of the plot and ΔL is the segment length (m).

Since the exiting sediment load at the start of the computation process is

approximated to determine the average sediment load, the computations are carried out iteratively till the exiting sediment flow values converge within 1 % of the relative difference. In case convergence does not occur within four trials the final exiting sediment flow is taken as the average of the last two computed values.

The expected value of the particle size distribution exiting each segment is also determined. Earlier, incoming sediment fractions for each particle size class are determined for each individual flow rate and its corresponding W/D value. In case of detachment, it is assumed that the particle size distribution remains unchanged. Changes in particle size distribution due to deposition are determined and are given by

$$fr_{[i,j,k]}^{(n+1)} = fr_{[i,j,k]}^{n} \left[\frac{1 - TE_{[i,j,k]}}{\left(1 - \sum_{i=1}^{i=b} TE_{[i,j,k]}\right)} \right] \qquad \text{(II.6.16)}$$

where $fr^{(n+1)}_{[i,j,k]}$ is the fraction of size i exiting segment number n, $fr^{n}_{[i,j,k]}$ is the fraction of particle size i entering segment n, $TE_{[i,j,k]}$ is the trapping efficiency for particle size i, b are the number of particle sizes under consideration and [j,k] are indexes of the channel flow rate and its respective shape.

The expected value of exiting sediment load for any particle size class is then determined by summation of all exiting loads for the size class across all the flow rates and their W/D values using the same computational procedure as used for determining the total expected deposition/detachment. In the same manner expected exiting loads are determined for other component particle size classes and the total exiting particle size distribution determined.

Evaluation over Complete Plot and Runoff event

Before initiating the computations, the plot is discretized into a selected number of segments, and the runoff event is also discretized into a given number of time steps. The number of segments and the number of time steps was decided based on sensitivity analysis of the model to each of the two parameters (discussed in Chapter II.7). As the number of segments and time steps were increased the computational time also increased; hence, an optimum value for both parameters was selected considering the effects on model results and the computational time. The filter was divided into chosen NSEG number of segments and computation made for NTI number of time steps. The incoming runoff hydrograph and the exiting runoff hydrograph were known for a given event from the field data collected. Assuming a uniform infiltration rate, total cross sectional runoff across each segment is determined. Actual distributions are input for the stochastic variables for each segment including channel density determined from the microtopography data and DEM analysis. Given the channel density and the total cross sectional runoff flow rate, distributions are determined. Using distributions of flow rates and the W/D values, channel shapes are defined for each segment at the start of the event, and are then updated for

subsequent time steps. Assuming sediment continuity down the filter, analysis is performed for all expected channel densities, flow rates and channel shapes across a section and extended for all sections down the plot. At the end of every time step, sediment flow exiting the filter and the particle size distribution for the sediment are determined.

The General Model

The general model was developed so that it could be applied to generic field situations where rainfall may occur on the filter strip and where the microtopography must be described probabilistically. The general model needs to take into account the dilution effect due to the added rainfall flow, since rainfall flows will enter channels carrying sediment laden runoff leading to increased transport capacity and decreased trapping efficiency. The major difference between the general model and the validation model was in the representation of stochastic parameters. The physically based approach was similar in both cases. Hence, only the major differences will be elucidated in this section.

Analysis was initiated by determining the possible channel density generated at a given segment due to incoming runoff and due to rainfall. Channels developed solely due to incoming runoff are defined as runoff channels 'n' whereas channels which are generated due to rainfall (neglecting the effect of incoming runoff) are defined as rainfall channels 'm'. The same definition is applicable to channel flows. Given the respective channel densities, conditional normalized flow distributions due to runoff ($p(q/q_{mean}|n)$) and rainfall ($p(q'/q'_{mean}|m)$ were determined. Thereafter, an algorithm was developed which allowed determination of conditional distributions for actual runoff and rainfall flow rates based on the parameters developed for normalized flow distributions (explained in the next section). Another algorithm was then developed to combine the two individual distributions to generate a probability distribution for the sum of the runoff and rainfall flows.

Since sediment was being transported and trapped in runoff channels, analysis of deposition was done for these channels only. Sediment flow in these channels was determined, taking into consideration the dilution effect of the addition of the rainfall flows. Hence for a given number of runoff channels, the probability distribution of the sum of runoff and contributing rainfall flows was determined and the probable channel shapes (W/D) for those flows was also determined.

The expected deposition could then be given by

$$E(D_p)=\sum_{i=1}^{imax} n_{[i]}p(n_{[i]})\sum_{j=1}^{jmax} p(q_{t[j]}|n,m)\sum_{k=1}^{kmax} p(W/D_{[k]}|q_{t[j]}).D_r(q_{t[j]},W/D_{[k]}) \qquad \text{(II.6.17)}$$

where $E(D_p)$ is the expected deposition, $n_{[i]}$ is the number of runoff channels $p(n_{[i]})$ is the probability associated with $n_{[i]}$, $q_{t[j]}$ is the total flow in the channel and $p(q_{t[j]}|n,m)$ its conditional probability and $p(W/D_{[k]}|q_{t[j]})$ the conditional probability for W/D given the flow rate $q_{t[j]}$.

ten runoff flows (where, $q_{i+1} = q_i + \Delta q$) and q'_1, q'_1, q'_3,.....q'_{10} (where $q'_{i+1} = q'_i + \Delta q'$) are the ten rainfall flow values, then the combined flow rates were determined as $q_{t1} = (q_1 + q'_1)$, $q_{t2} = (q_1 + q'_2)$, $q_{t3} = (q_1 + q'_3)$,....., $q_{t100} = (q_{10} + q'_{10})$. As per the above equation each of the ten incremental rainfall flow values were further subdivided for determining probability of the total flow values.

Channel shape (W/D)

Computation of probability distributions corresponding to normalized W/D values were similar to the approach used in the validation model except that the W/D values were for the combined channel flows (runoff + rainfall) as opposed to runoff flows only.

Sediment Routing

Similar to the approach used in the validation model, sediment concentration was calculated at the midpoint of every segment using equation II.6.1 and partitioning among flows by equation II.6.2. The calculation of the partition coefficient (K_r) for equation II.6.2 was made considering the contribution of rainfall flow to the total flow exiting the segment. Since the rainfall volume is added down the filter to the total runoff across each section, this additional rainfall has a dilution effect and lowers the sediment concentration. Hence the value of K_r for the $n+1^{th}$ segment is given by

$$K_r^{n+1} = \frac{Q_{so}^{'n}}{Q^{n+1} + \left[\sum q' . p(q'|m)\right]^{(n+1)}} \qquad \text{(II.6.20)}$$

where Q_{so}^n is the sediment load exiting the nth segment, Q^{n+1} is the total runoff flow entering the $n+1$ segment, q' is the rainfall flow, m is the number of rainfall rills/channels and $p(q'|m)$ is the conditional probability for q' given total number of m channels.

Physically Based Processes

The framework for modeling of the physically based processes, such as transport capacity, deposition/detachment, channel shape, sediment load, and particle size distribution were similar to the approaches used in the validation model.

An additional computation that was required in the general model was the computation of the runoff generated due to rainfall on the filter. The runoff was determined by assuming a uniform infiltration rate across the full length of the filter. This infiltration rate was determined based on the infiltration observed for incoming runoff during experimental runs.

Stocha

genera
Binomi
Gamm
Hence,
averag
across

Chann

flow ra
rainfall
runoff
distribu
genera

where
the nu
above

is give

where
probab
is the i
consid

increm
flow va
each in
genera
a total
was de

Execution of the Model Over the Complete Plot and Storm Event

The general model is executed over the complete filter length and sto as shown in Figure II.6.1. Similar to the validation model, the filter plot wa into NSEG number of segments and NTI number of time steps. Total cross flow across each segment was determined assuming uniform infiltration fo length of the plot. Probabilities for runoff and rainfall channel densities were g using fitted binomial distributions. Similarly, pdfs for combined flows were g using fitted gamma distributions of runoff and rainfall flow. Pdfs for W/D valu also developed from gamma distributions. Sediment continuity was assum the filter, and sediment concentrations for each segment were determined b the sediment concentration exiting the upslope segment and the dilution expe to addition of rainfall flows. The analysis was made over all the time steps to expected exiting sediment flows and sediment particle size distribution from for each time step.

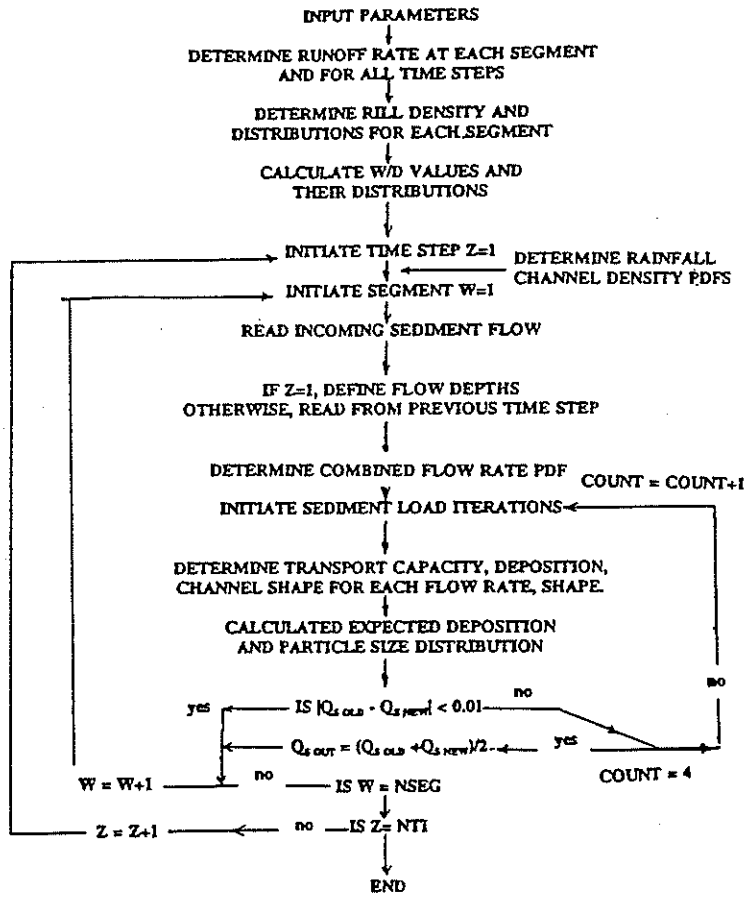

Figure II.6.1. Complete Flow Chart for the General Model.

CHAPTER II.7

MODEL VALIDATION AND SENSITIVITY ANALYSIS

Model Validation

The sediment trapping model for the riparian grass filters was evaluated using data collected and developed from field observations. Since actual values were unknown, initial estimates for input variables such as Manning's n and critical tractive force were taken from literature for which model results were determined. Predicted results were them compared to the observed to determine the optimum value of the input parameters. Actual values of channel density and their distributions for each section down the plot were input as opposed to using probability density functions (pdfs) of channel density fitted to data across all the plots. Similarly, distributions for flow rates and W/D ratios developed from observed data were input as opposed to using pdf's determined from fitted distributions.

Parameter Selection

The grass filter model needed a number of input variables, some of which were developed from field data and some of which were estimated. The values obtained from field observations derived from literature are

- *Bulk density:* Bulk density measurements for tilled topsoil were made on a similar soil in a previous study (Storm et al., 1991) with a range of values between 1025 - 1090 (kg/m^3). A value of 1090 was initially selected for this analysis. Further evaluation indicated that a higher value would be appropriate, since the filter was not filled, but selection of the bulk density value was not critical to model results as determined later in the sensitivity analysis.

- *Eroded particle size distribution:* Incoming and exiting eroded aggregate particle size distributions were derived from experimental observations.

- *Grass spacing:* Spacing of grass media was determined experimentally and was found to be 0.0127 m. This observed value was less than the values of 0.015 - 0.020 m reported in earlier studies (Hayes et al., 1979).

- *Ground slope:* Ground slope was measured experimentally and found to be an average of 0.087 across all the plots.

- *Depth to non-erodible layer:* A value for the depth to non-erodible layer was derived from earlier studies (Lewis et al., 1991) and found to be 0.16 m. Again this estimated value did not affect the model predictions as detachment on bare soil in grass filters was mostly absent in model simulation as well as on field filter runs.

- *Critical tractive force and rill erodibility coefficient:* Values for critical tractive force and rill erodibility coefficient were derived from earlier studies done on similar type of bare soil (Lewis et al., 1991). The critical tractive force for bare top soil was assumed as 3.2 N/m^2, from which tractive force under grassed conditions was determined. The value for rill erodibility was estimated to be 0.00125 s/m. Estimated values of critical tractive force and rill erodibility coefficient did not influence validation results as detachment of parent bed material was not observed on experimental plots and was also not observed during model runs.

- *Debris depth:* Debris depth represents the depth of the grass debris between the grass media. Based on visual observations it is estimated that this parameter may vary between 0.00635 m to 0.0127 m and thus was assumed to be 0.012 m.

- *Manning's n:* An initial estimate of Manning's n for dense turf grass was taken from literature (Barfield, Warner, and Haan; 1983). Manning's n values of 0.35, 0.3 and 0.2 were also evaluated for model prediction. Of the three values the value that gave the closest prediction of results for all the plots was 0.35. The values were larger than those measured by Hayes (et al., 1979) for laboratory studies of flow. The Hayes values were for flows with the flow depths of the order of 0.05 to 0.10 m, whereas the flow depths observed for this study were of the order of 0.01 m.

The values of the above discussed parameters are listed in Table II.7.1.

Table II.7.1. Physically Based Input Parameters for Model Validation

Parameter	Symbol	Unit	Value
Segment Length	SLEN	m	0.3048
Time Step	DELT	secs	600
Number of Discrete Flow Rates	JMAX	-	40
Bulk Density	BDEN	kg/m^3	1090
Depth to Non-Erodible Layer	DNE	m	0.16
Manning'n	RMANN	-	0.35
Grass Spacing	GRASPAC	m	0.0127
Debris Depth	DEB	m	0.012
Sediment Averaging Coefficient	THETA	-	0.5

Validation Results

Model validation was performed with data from six plots over a total of nine of 12 storm event runs. In three of the total 12 storm event runs, either there was no exiting runoff from the filter or the runoff was so small that suitable comparison of predicted and observed values could not be made. Each of the filter plots was discretized down the slope into segments of 0.3048 m, a value which was determined by performing sensitivity analysis (to be discussed in detail later). The model was found to be sensitive to the segment length, but as the segment length was reduced the sensitivity curve flattened out. The selected segment length of 0.3048 m was in this flat region of the curve which ensured that the model predictions were relatively insensitive to segment lengths. The time increment used for analysis was 600 seconds (10 minutes) which was the minimum interval for which the inflow and outflow runoff values were computed. The inflow and outflow runoff hydrographs and sedimentgraphs for each of the plots were measured as described in Chapter II.4. These hydrographs and sediment graphs were filtered before input into the program to remove small fluctuations. In grass filters this filtering effect occurs as a result of backwater effects and the buffering ability of the grass media. The number of discrete flow rates considered for analysis was 40. This number was found optimum considering the sensitivity of the model and also the computational time required.

For each of the plots, actual values for rill/channel densities derived from the DEM analysis were input for each section down the plot. For example, the channel density at the top most section for plot four (run one) was five and the probability corresponding to five rills/channels was input as 1.0. Distributions for flow rate and W/D values used were those that were developed from data, as opposed to the pdfs generated by fitted distributions (Gamma) to data.

Selection of Manning's n

Since the actual values for Manning's n are not known, model predictions were determined for Manning's n values of 0.2, 0.3, 0.35 and 0.4 for channels in the filter media. A validation statistic 'VS' was developed to compare the observed and predicted exiting sediment flow across the duration of the storm event and to determine the optimum value of Manning's n. The value of VS (an absolute value) was determined as

$$VS = \frac{1}{n} \sum_{i=1}^{n} \left| \frac{q_{spi} - q_{soi}}{q_{soi}} \right| \qquad \text{(II.7.1)}$$

where q_{spi} is the predicted exiting load, q_{soi} is the observed exiting load, n is the number of points on the predicted sedigraph, and the brackets imply absolute values. The validation statistic was a measure of the difference or error between the predicted and observed exiting sediment flows. A low value of VS signifies an closer prediction by the model to the observed values whereas an high value of the VS signifies a greater variation. The validation statistic was then averaged for all the conventionally

tilled erosion plot setups to give the average error (AE). This average error was expressed as

$$AE = \frac{1}{m} \cdot \sum_{j=1}^{m} VS_j \qquad \text{(II.7.2)}$$

where m is the number of filter plots under consideration and VS_j is the validation statistic for a given filter plot. AE values were determined for each of the selected Manning's n values as shown in Figure II.7.1. As in the case of VS, a smaller AE value signifies closer model prediction to the observed data. As can be seen from Figure II.7.1 the lowest value of AE was found for a Manning's n value of 0.35. Hence a Manning's roughness value of 0.35 was chosen as the optimum value for validation runs.

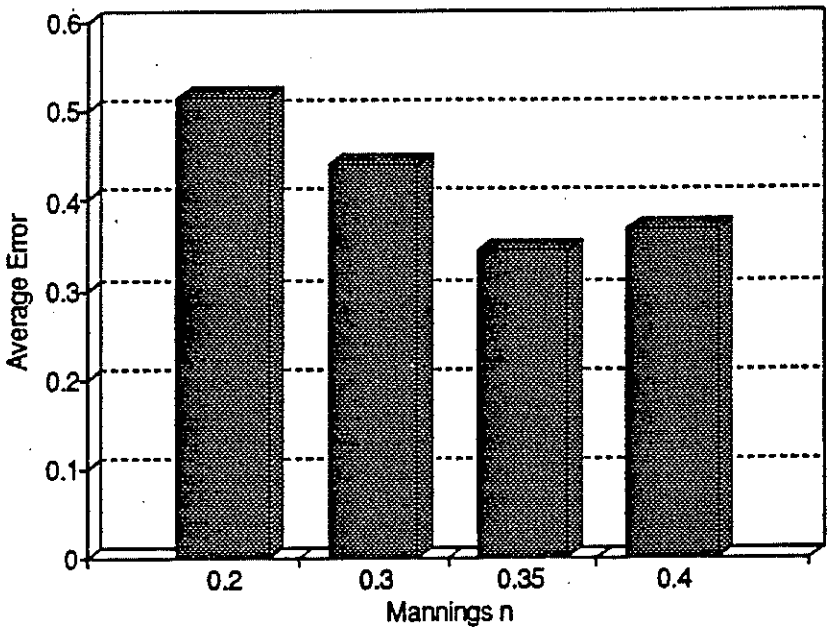

Figure II.7.1: Average Error Values (AE) Corresponding to Each Manning's n Value.

Comparison of Trapping Efficiencies

The first evaluation to be made is in prediction accuracy for trapping efficiency, or the mass retained in the filter. The results are as shown in Figure II.7.2, indicating that the model does an excellent job of predicting trapping efficiency. The average error in trapping efficiency over all plots was 0.99%. This successful prediction indicates that the model is adequately representing the cumulative effect of the distribution of mass between settling and infiltration.

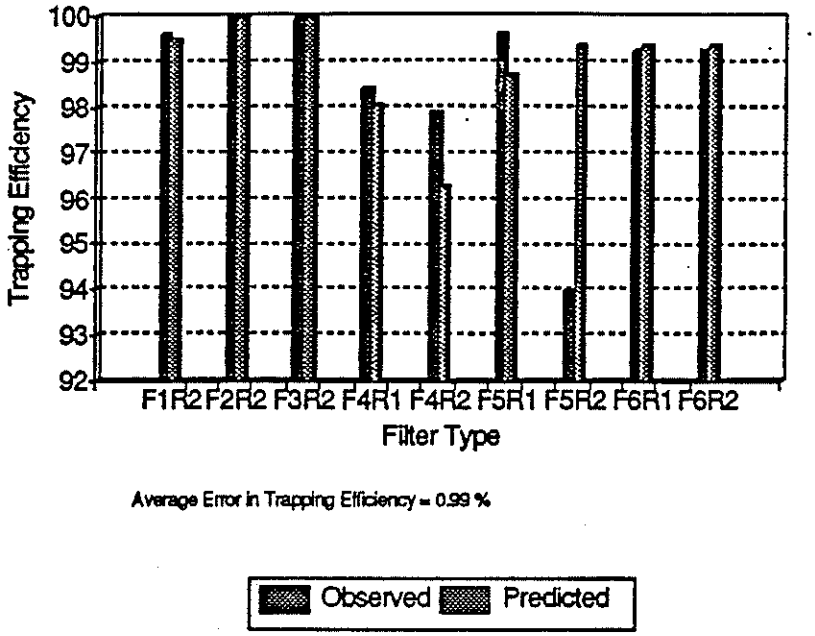

Figure II.7.2: Comparison of Observed and Predicted Trapping Efficiencies.

Comparison of Predicted and Observed Exiting Sedigraphs and Particle Size Distribution

A summary of the observed and predicted parameters with erosion plot and filter strip characteristics is given in Table II.7.2. Comparison of the predicted and observed sedigraphs and the exiting particle size distributions across all the plots for a Manning's n of 0.35 are given through Figures II.7.3 to II.7.18. Predicted exiting particle size distributions in the figures are expressed as t1, t2, t3 (t1, t2, t3 are the first, second and third points on the storm duration) and observed curves are expressed as obs1, obs2. The model gave a good prediction of exiting sediment flow for plot four (runs one and two) for a Manning's n of 0.35. For plot four a 15 foot filter, the incoming sediment load generated off a conventionally tilled erosion plot was high. Exiting sedigraph for run two of plot four indicates a sudden jump which is a questionable data point, because the trend does not continue beyond that particular observation.

The model did not predict accurately for plot five (runs one and two) for which the incoming sediment was generated off a minimum tillage erosion plot. The model underpredicted the trapping for the first storm event (plot five) but then overpredicted it for the second one. During field observations it was observed that a large amount of plant debris was washed onto the filter from the minimum tillage erosion plot. Observed exiting sediment graph for plot five, run two indicates a sudden jump in the exiting sediment flow which the model failed to simulate. The reason for the lack of agreement is not clear. The model predicted greater exiting sediment load for run one of plot five but lesser for run two.

Table II.7.2. Summary of Validation Results

Plot #	Run #	Tillage Condition	Filter Length	Erosion Plot Runoff Avg.	Filter Runoff A vg	Erosion Plot Sed. Yield	Filter Sed. Yield	Filter Trapping Eff. (AVG) OBS	Filter Trapping Eff. (AVG) Model	% Infilt. into Filter
1	1	CONVEN	30.00	.07	0.0	52.80	0.00			100.00
	2		30.00	1.16	0.0	247.20	1.25	99.5	99.5	91.76
2	1	MINIMUM	30.00	.01	0.0	3.20	0.00			100.00
	2		30.00	0.58	0.0	19.96	0.00	99.9	99.9	99.53
3	1	MINIMUM	45.00	0.09	0.0	0.80	0.00			100.00
	2		45.00	.07	0.0	12.91	0.00	99.9	100.0	98.18
4	1	CONVEN	15.00	0.98	0.1	106.62	3.01	98.3	98.0	87.86
	2		15.00	1.31	0.1	268.14	9.39	97.8	96.2	88.70
5	1	MINIMUM	15.00	1.35	0.0	56.19	0.20	99.6	98.7	94.36
	2		15.00	1.21	0.1	70.05	4.37	93.9	99.36	90.91
6	1	CONVEN	45.00	1.29	0.0	268.59	2.12	99.2	99.34	93.00
	2		45.00	1.49	0.1	342.28	2.42	99.2	99.34	93.09

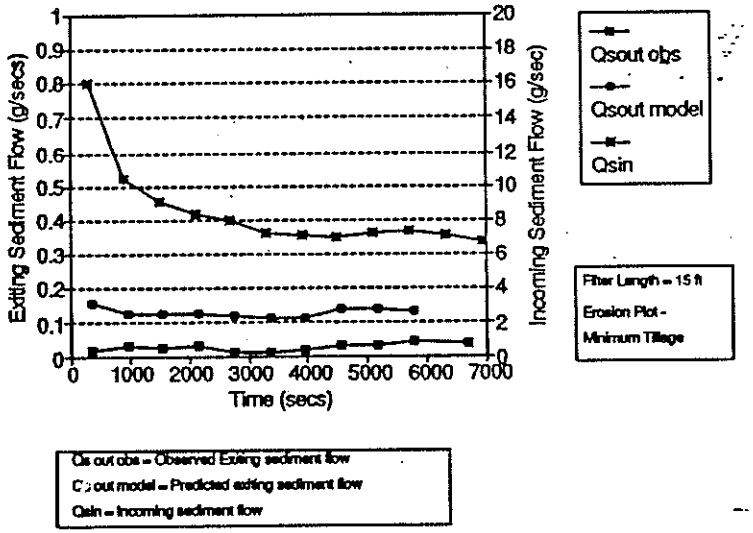

Figure II.7.7 Exiting Sediment Flow for Plot 5 (Run 1).

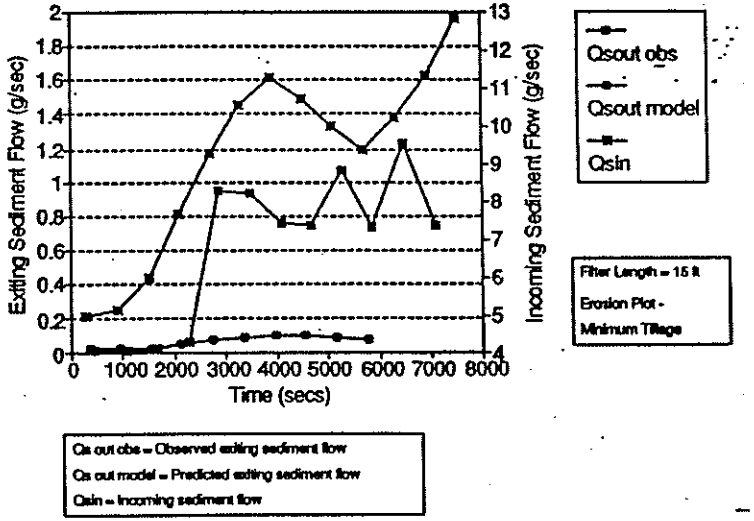

Figure II.7.9. Exiting Sediment Flow for Plot 5 (Run 2).

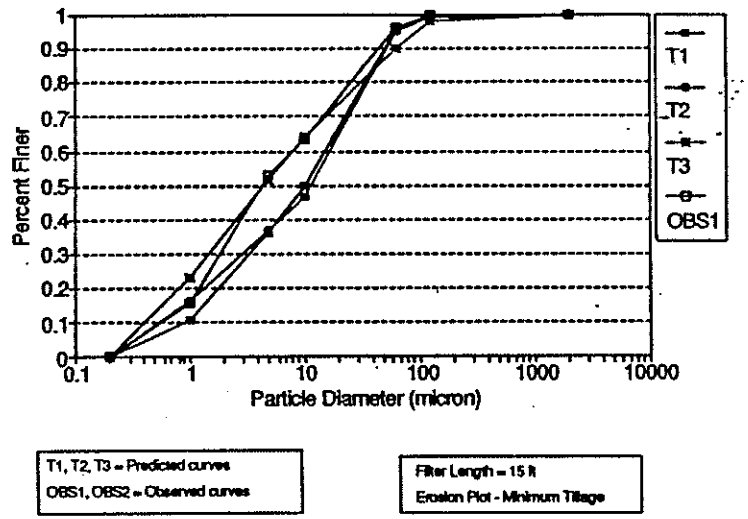

Figure II.7.8. Exiting Particle Size Distribution for Plot 5 (Run 1).

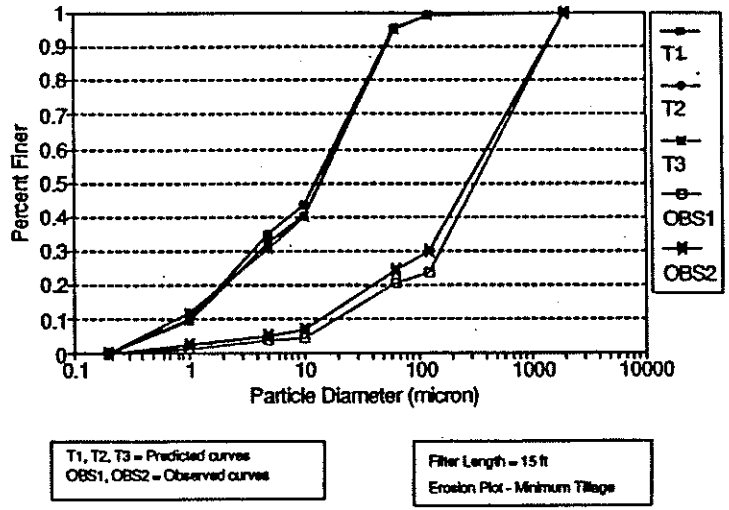

Figure II.7.10. Exiting Particle Size Distribution for Plot (Run 2).

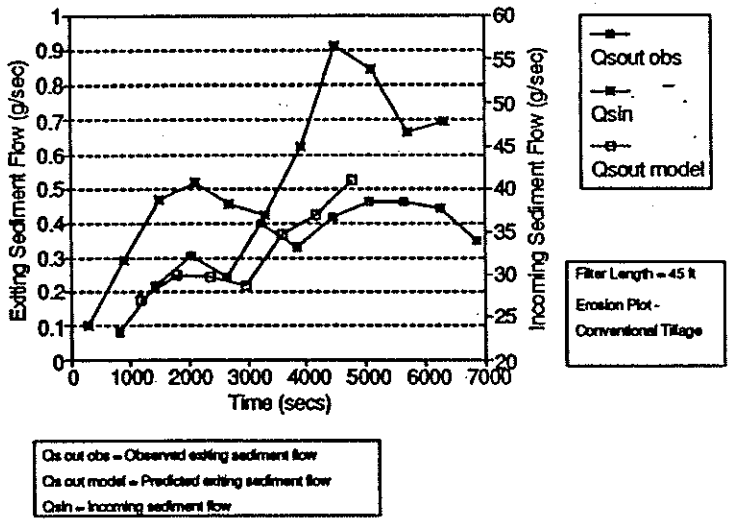

Figure II.7.11. Exiting Sediment Flow for Plot 6 (Run 1).

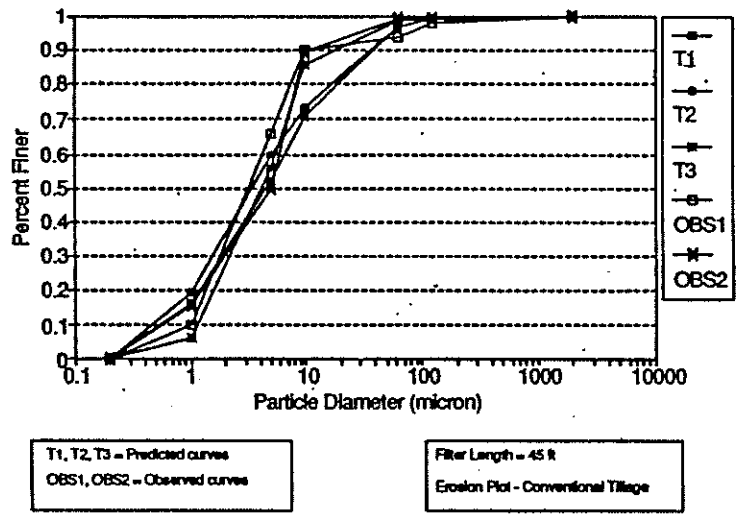

Figure II.7.12. Exiting Particle Size Distribution for Plot 6 (Run 1).

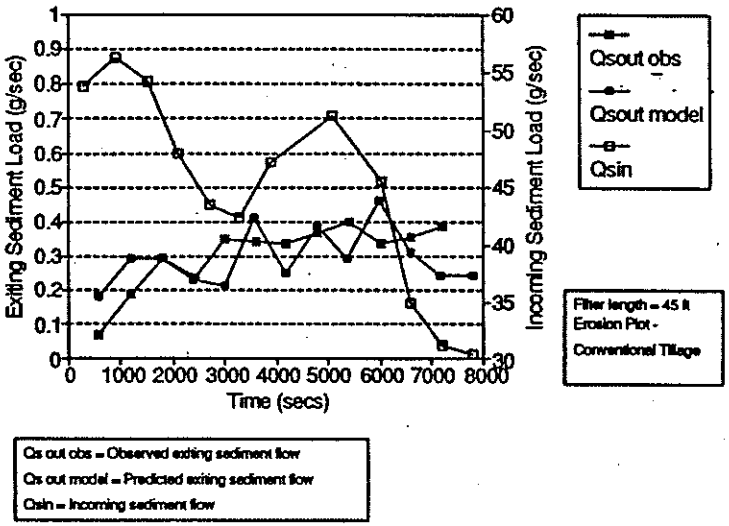

Figure II.7.13. Exiting Sediment Flow for Plot 6 (Run 2).

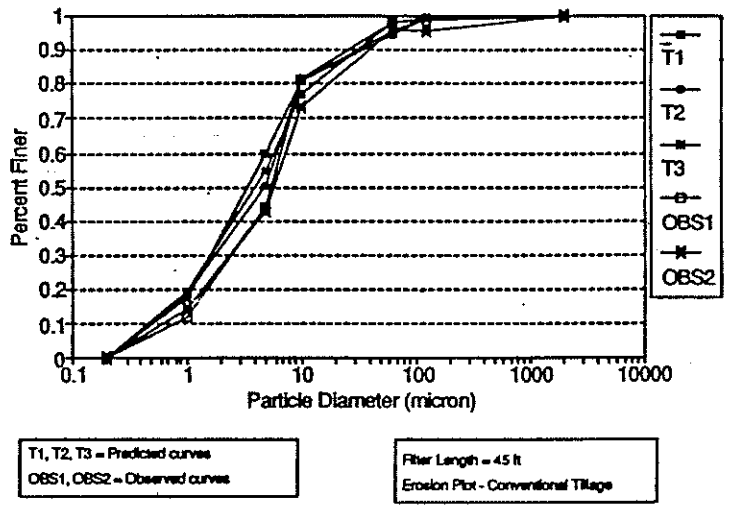

Figure II.7.14. Exiting Particle Size Distribution for Plot 6 (Run 2).

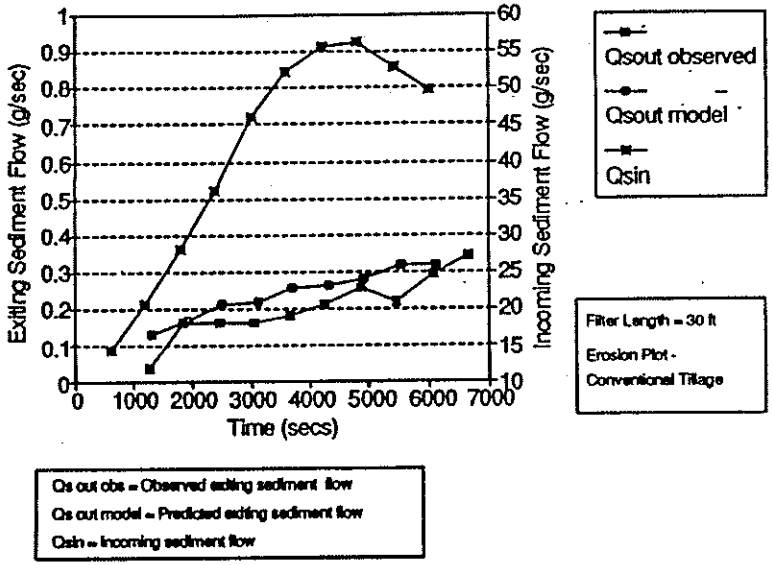

Figure II.7.15. Exiting Sediment Flow for Plot 1 (Run 2).

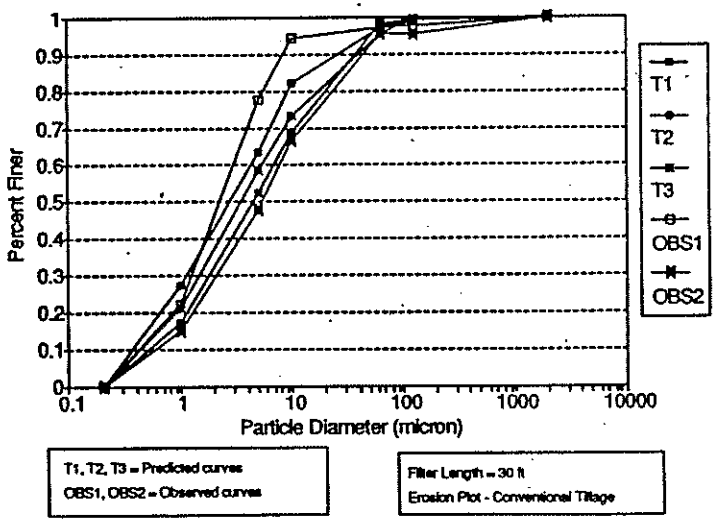

Figure II.7.16. Exiting Particle Size Distribution for Plot 1 (Run 2).

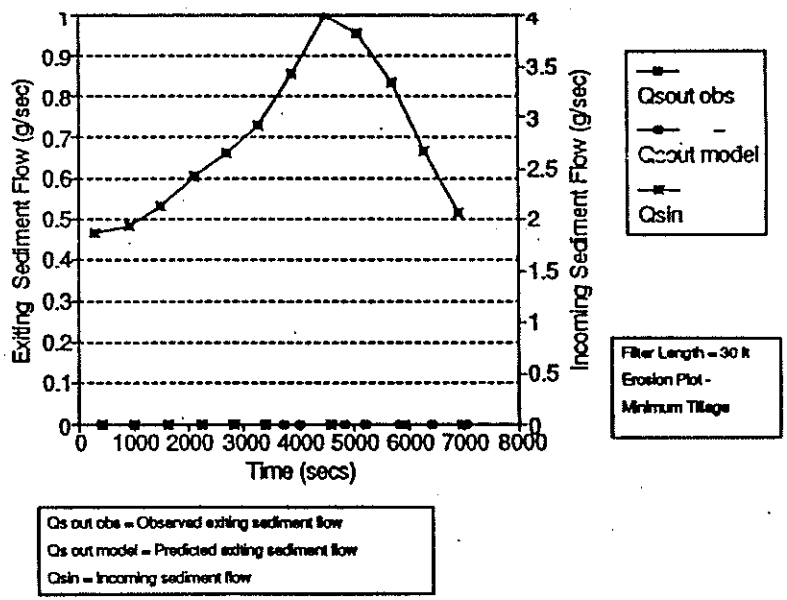

Figure II.7.17. Exiting Sediment Flow for Plot 2 (Run 2).

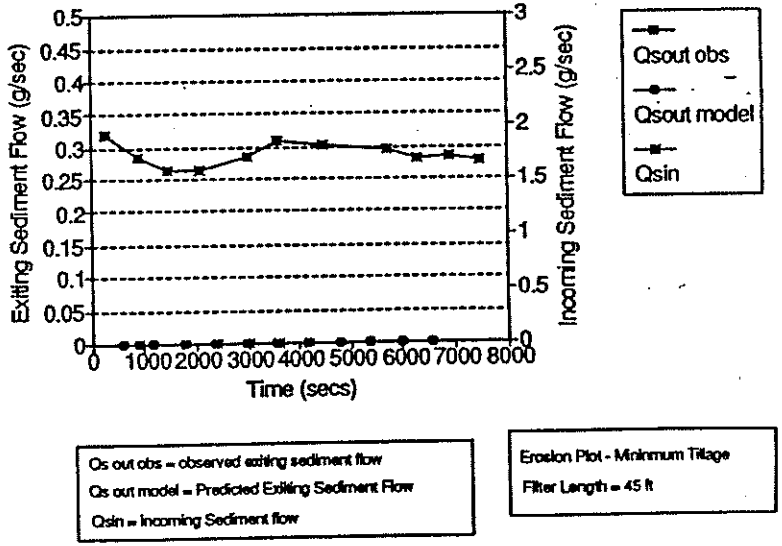

Figure II.7.18. Exiting Sediment Flow for Filter Plot 3 (Run 2).

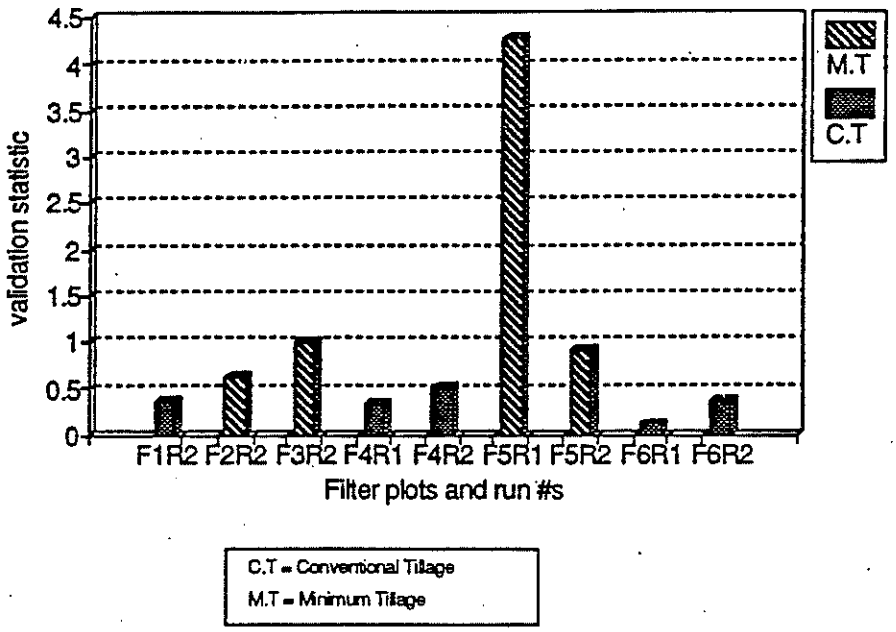

Figure II.7.19. Exiting Sediment Flow Validation Statistic for Each Filter Plot. F indicates the filter plot and R the run number.

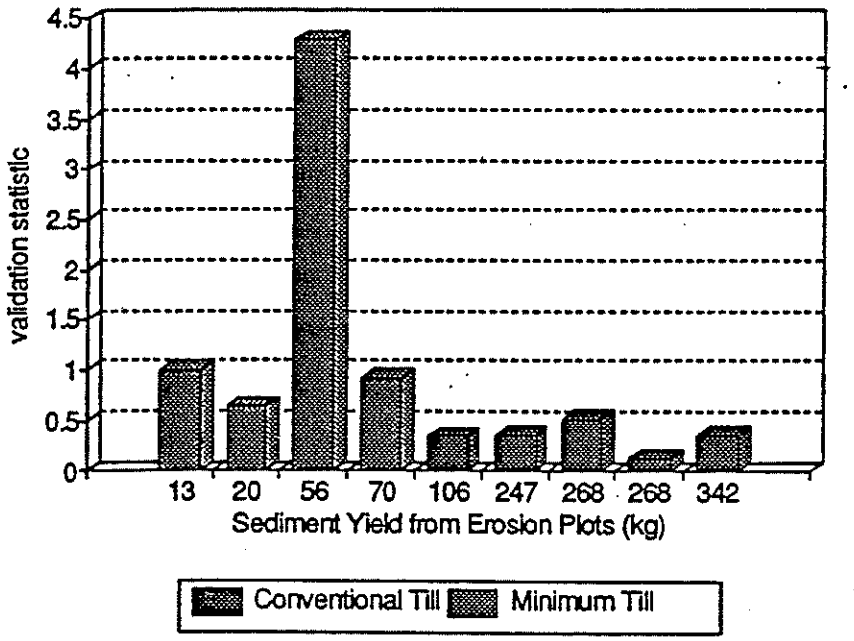

Figure II.7.20. Variation of Exiting Sediment Load Validation Statistic with Sediment Yield.

The model gave a good prediction of exiting sediment flow for filter plots one, two and six. Model evaluation for plot one and two was restricted to the second storm event run as the first events had failed to produce any runoff off the filter. Observed and predicted sediment trapping efficiencies for plot six, a 45 foot filter, was lower than that of plot three, another 45 foot filter. This may be attributed to the high amount of runoff and high incoming sediment flow observed for plot six. Observed exiting sediment flows from plots two and three were small as the model predictions also indicated.

Two observations need to be made about the plots in Figures II.7.3 through II.7.18. First of all, the scale for the incoming and exiting sediment flows are on different axes. Typically, exiting sediment flows are an order of magnitude less than incoming flows. Secondly, although the actual magnitude of predicted and observed exiting flows are different for plots five, the difference is small compared to the incoming sediment load. This is indicated by the excellent agreement between predicted and observed trapping efficiencies in Figure II.7.2.

Validation Statistic

The performance of the model in predicting overall trapping during the storm was evaluated by trapping efficiency and found to be excellent. The performance of the model in predicting point to point exiting sediment flows can be determined from the validation statistic in equation II.7.1. Validation statistic values are plotted against the erosion plot condition and the filter length as given in the Figures II.7.19 and II.7.20. As can be seen from the figures, conventionally tilled erosion plots had higher sediment yields and had low corresponding VS values indicating better model prediction, whereas no till or minimum tillage erosion plots had high VS values. The deduction that can be made from this result is, that the model predicted more accurately (closer to the observed values) when there was sufficient sediment in the flow as compared to when the sediment inflow was low. Runoff generated off no till or minimum tillage plots had a large fraction of plant debris which in some cases was greater than the sediment fraction.

It is important to point out that putting excessive weight on validation statistic results can be misleading. Although these statistics indicate the relative prediction accuracy for instantaneous exiting sediment flows, a high value does not automatically invalidate model usefulness. For example, with the exception of plot five, the predicted and observed peak exiting sediment flow rates compared favorably as shown in Figure II.7.21. This along with the total sediment load discharged is the most important statistic.

Other Observations.

The percentage of infiltration for each grass filter was also determined and is given in Figure II.7.22. This was done to determine the effect of filter length on the total amount of infiltration. As can be seen from Figure II.7.22 a general increasing trend in the percent infiltration can be seen with increasing filter lengths which is what one would have expected.

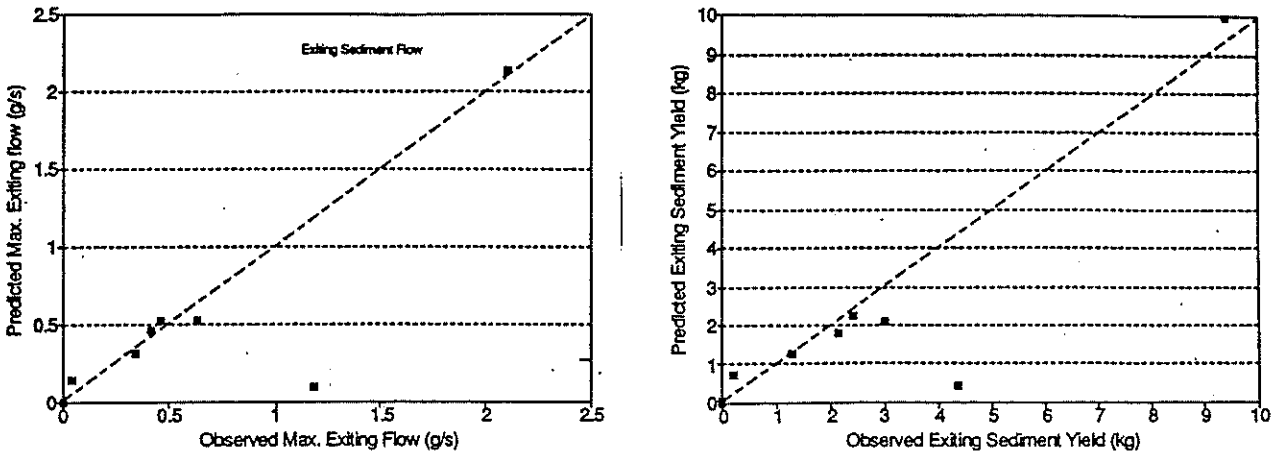

Figure II.7.21. Comparison of Predicted and Observed Maximum Instantaneous Sediment Flow and Sediment Yield.

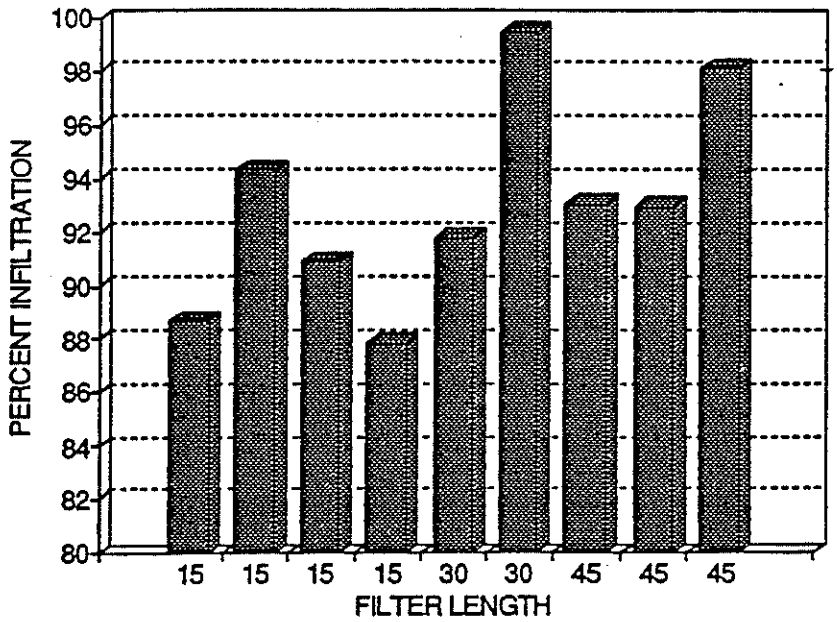

Figure II.7.22. Percent Infiltration for Different Filter Lengths.

A consideration that needs to be taken into account when analyzing these results is that these trapping efficiencies are determined using channel density generated by the DEM model. As discussed earlier the DEM model does not allow bifurcation of flow, whereas in actual filter plots this phenomenon (bifurcation of flow from a single channel into two or more) was observed frequently. Bifurcation of flow increases the number of channels at a section thus, increasing the trapping at that point. Hence the model may give conservative estimates of trapping in a condition where the grass filter plot is on a gentler slope where partitioning of flow may occur at the down slope end of the filter.

Conclusions About Validation

Model predictions for trapping efficiencies of grass filter plots matched closely with those observed for a optimum Manning's n of 0.35. The percent variation between observed and predicted trapping efficiencies was within 2% for most of the filter plots. The predicted exiting particle size distributions were also within reasonable accuracy. Exiting sedimentgraph shape showed a good correlation with the shape of the exiting runoff hydrograph. The predicted and observed instantaneous maximum sediment flow and the sediment yield were also compared and were found to be in good agreement with the exception of one point. These results indicate that the model has validity. Although the model was capable of handling detachment, only deposition conditions occurred over all the flow rates during the storm event. This was expected as the incoming sediment load was much higher than the sediment transport capacity in the filter. The model gave more accurate predictions of instantaneous exiting sediment flows when the sediment fraction in the incoming runoff was high, which was the case when the runoff was generated off a conventionally tilled erosion plot. In contrast, model predictions for instantaneous exiting sediment flows were less accurate when the runoff was generated off a no till or a minimum tillage plot with a large fraction of plant debris and a small sediment fraction in the runoff.

Validation results and field observations showed that the trapping efficiency of the filters did not increase proportionately with the increase in the filter length. The trapping observed for the 45 ft filter length was only slightly more than that observed for the 15 ft filter length. Though the difference in trapping for a single storm event may not be large for the 15 and 45 ft filter, the longer filter has a greater storage capacity and may have a better filtering effect over a long period of time or over a number of storm events. Sediment buildup up to the bottom edge in the form of deltas occurs earlier for shorter filters thus leading to greater transport of sediment through the filter. This situation was considered in the model by differentiating the deposition phenomenon into two conditions - deposition with insufficient sediment deposited thus transport unavailable, and deposition with sufficient sediment deposited and transport available. Model evaluations did indicate that more and more numbers of channels attained the latter condition of deposition earlier in case of a shorter filters. For subsequent storm events on the filters (run two) the predicted and observed trapping efficiencies seemed to decrease, which could be attributed to increased runoff (see Table II.7.2) and greater channelization of flow. Also, sediment deposited in the filters from prior storm event runs could have reduced the infiltration by

clogging/covering the macropores in the filter. DEM generated channel networks after every event did indicate that for longer filters, channelization of flow was increased as sediment build up occurred in the filter.

Sensitivity Analysis

A sensitivity analysis of the model was done to determine model response to changes in input parameters and whether such responses could be physically explained. Sensitivity of the model was determined for three types of parameters - discretization parameters, physically based parameters and stochastic inputs.

The sensitivity analysis was done using data from filter plot four, run one, as a base condition. A single parameter sensitivity analysis was conducted using this base in which a given single parameter was varied to predict model sensitivity. The parameter chosen for evaluating sensitivity was sediment trapping efficiency (averaged over the storm event). Trapping efficiency was chosen since this is the parameter that is generally used to represent the efficacy of a grass filter.

Discretization Parameters

Sensitivity to discretization parameters such as segment length, time increment, and discrete flow rates had to be determined before model validation could be performed. The effort was to define the filter plot and the storm event with as many discrete elements as possible so that it enhanced computational accuracy but also did not negatively influence computational efficiency.

Segment Length. As discussed before, filter plots were discretized into segments of equal length for analysis model. Sensitivity analysis to segment length is shown in Figure II.7.23. The model is sensitive to segment length in spite of the fact that a correction factor for length was included in the model. The segment length is used in a number of equations in the model such as determination of fall number for computing deposition. Segment lengths of 1.524 m, 0.9144 m, 0.5715 m and 0.3048 m were the initial trials. A small segment length was preferable for greater accuracy. But, as the plot was discretized into greater number of segments computational time increased. Sensitivity analysis indicated that the sensitivity of the model to segment length decreased for segment length less than 0.5715 m, hence a segment length of 0.3048 m was chosen for the validation runs. For the sensitivity analysis a segment length of 0.3048 m required inordinately long computational time (around 45 to 50 minutes) hence a segment length of 0.9144 m was chosen.

Incremental Time Step. For accuracy it was desirable to have the minimum time increment available. Data measurements for runoff and sediment flows were done at every 10 minute intervals, hence 10 minutes (600 seconds) was the minimum time increment available and thus was chosen. Model sensitivity was determined for time increments of 600, 1200 and 1800 secs and is as shown in Figure II.7.24. This indicated that the model was relatively insensitive to the time step.

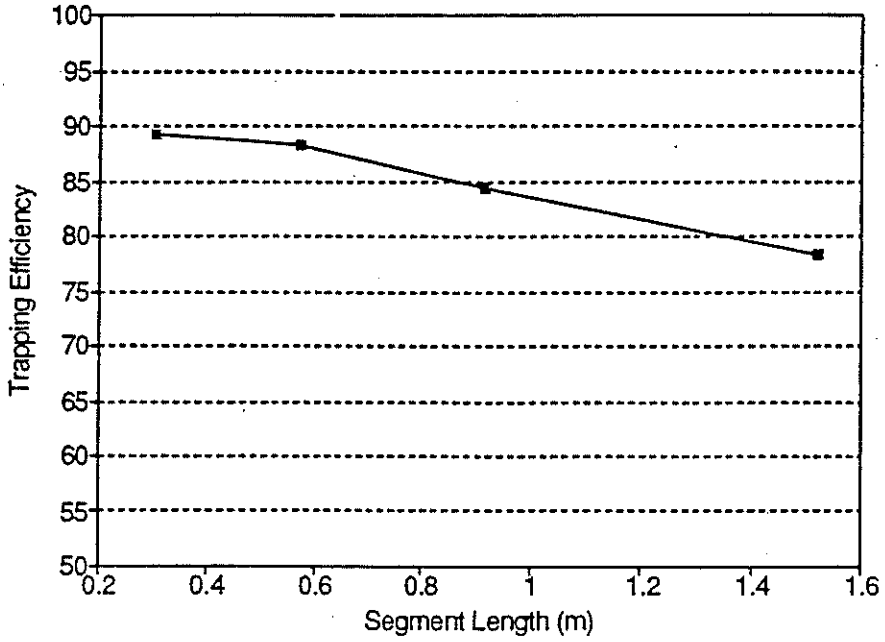

Figure II.7.23. Sediment Trapping Efficiencies for Different Segment Lengths.

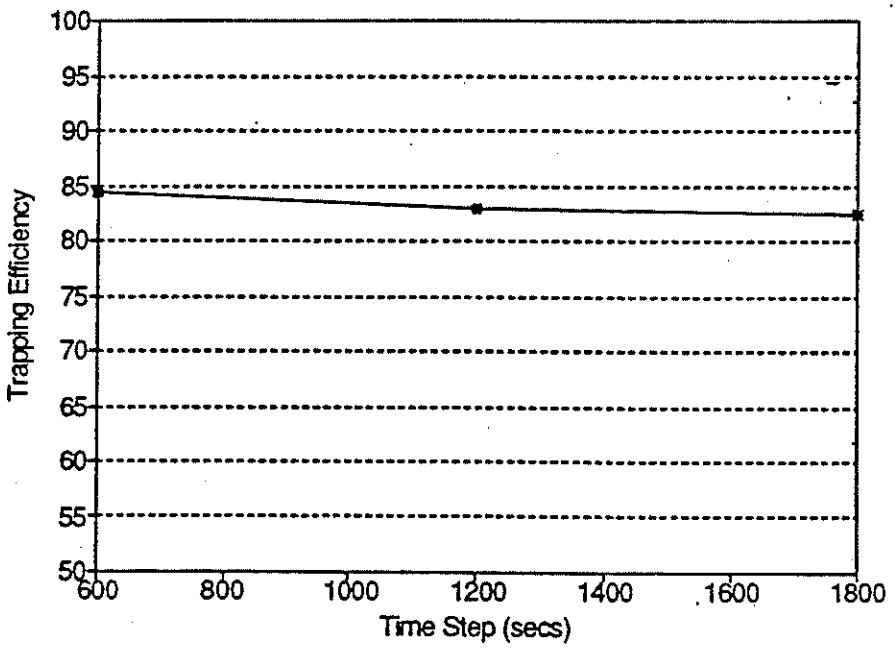

Figure II.7.24. Sediment Trapping Efficiencies for Different Time Increments.

Discrete Flow Rates. It is desirable to have the maximum number of discrete flow values so that a complete representation of probability distribution can be achieved (Lewis et al. 1991). Increasing the flow rates also increases the model computational time. For the general model the number of discrete flow rates chosen was 100 as that was the maximum the model could handle considering run time requirements. In case of the validation model this optimum value was restricted to 40, based on an analysis that indicated increasing the number beyond 40 had little impact on prediction.

Physically Based Non Discrete Parameters. Physically based non discrete parameters included ground slope, Manning's roughness coefficient, debris depth and bulk density. Parameters such as critical tractive force and rill erodibility were not included as detachment conditions were not observed during the run. The specific parameter under consideration was varied by +10% and -10% from the baseline value (used in the model validation) with other parameters remaining same. The sensitivity for physically based non discrete parameters was determined using a non-dimensional statistic (Lewis et al., 1991) given as

$$S=\left(\frac{BV}{R(BV)}\right)\frac{R(BV+10\%)-R(BV-10\%)}{(BV+10\%)-(BV-10\%)} \qquad \text{(II.7.3)}$$

where BV is the base line value and R(BV) is the resultant trapping efficiency corresponding to the baseline value. The results for each of the parameters are as shown in Table II.7.3.

Table II.7.3. Sensitivity Results for Physically Based Non Discrete Parameters

Sensitivity Parameter	Value	Trapping Eff.	Sensitivity Statistic
Manning's n			0.0549
	0.385	84.74	
	0.325	83.98	
Debris Depth			0.00537
	0.0132	84.34	
	0.0108	84.24	
Bulk Density			0.0000
	1199	84.33	
	981	84.24	

Trapping Efficiency for Base Conditions = 84.32

Manning's n significantly influences trapping efficiency by reducing the flow velocity thus allowing more time for sediment particles to settle to the bottom. An increase in the roughness leads to an increase in the trapping efficiency as reflected in the observed sensitivity statistic.

Ground slope is one of the parameters that has the most influence on the model results. A large variation in the ground slope can lead to a change in the channel density distributions down the plot as the flow gets more channelized with increasing slope. This can also lead to a different distribution of flow rates in the channels, and thus also affect the probability distribution of channel shapes. The probability distribution of channel density, flow rates and channel shapes can be expected to be vastly different for a slope of 10% as compared that for a slope of 40%. For an increase in slope an increase in exiting sediment load can be expected accompanied with a coarser exiting particle size distribution. The model does predict a coarser size distribution for a 10 % increase in the slope as shown in Figure II.7.25.

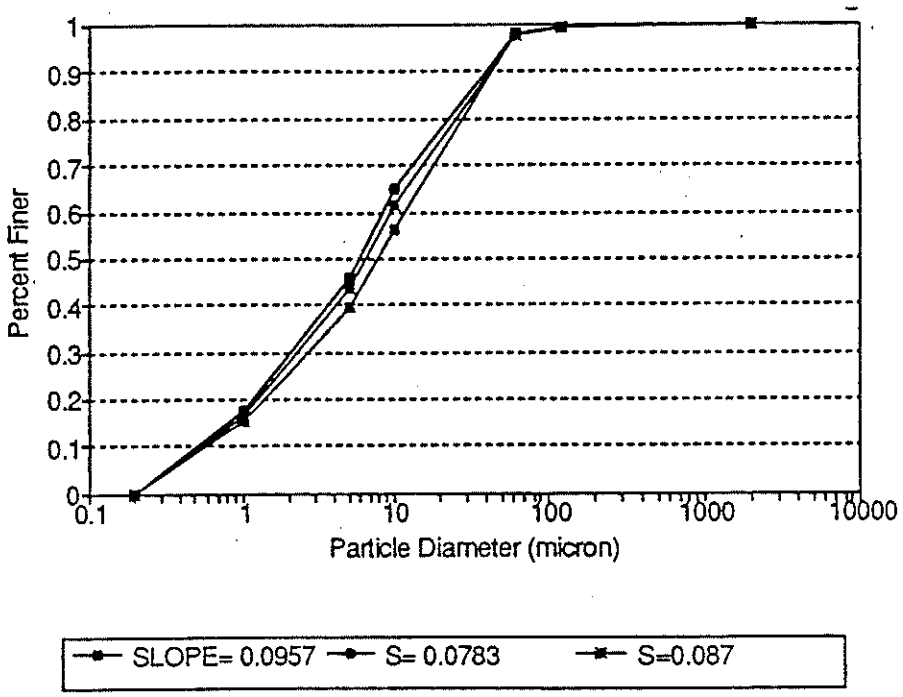

Figure II.7.25. Particle Size Distribution Reflecting Sensitivity of Model to Ground Slope

Debris depth is the thickness of grass debris deposited in between the grass media. From experimental observations it was observed that this may vary between 0.0063 to 0.0127 m, hence a value of 0.012 m was selected. Further research needs to be conducted to determine an accurate value for this parameter. From sensitivity results it was observed that the model was not particularly sensitive to this parameter, as shown in Table II.7.3.

The model was not sensitive to bulk density under given input conditions. Since this parameter comes into play only when detachment is occurring. No detachment was occurring in this storm run.

Physically based discrete parameters selected for evaluation were mean channel/rill density, particle size distribution, rainfall intensity and incoming rainfall rates and rainfall infiltration rate. Sensitivity to these parameters was determined by determining the relative difference between the average trapping efficiencies (averaged over the duration of the storm event) given the modified parameters and the average trapping for the baseline parameters. The sensitivity results for these parameters is given in Table II.7.4.

As discussed in an earlier chapter, uniform flow through the filter is represented by infinite number of channels/rills placed close to each other. Hence as the mean channel density increases at a section greater trapping can be expected. The mean channel density at each of the sections was varied from 2 to 4. The model is sensitive to the mean channel density as shown by the results.

Table II.7.4 Sensitivity Results for Physically Based Discrete Parameters

Sensitivity Parameter	Value	Trapping Efficiency	Percent Difference
Trapping Efficiency for Base Conditions = 84.32			
1) Mean Rill/Channel Density			
	2	82.45	-2.20
	4	87.75	4.06
2) Particle Size Distribution			
	10%+	84.48	0.191
	10%-	81.80	-2.99
3) Rainfall Intensity and Runoff Rates			
	10%+	82.81	-1.79
	10%-	86.52	2.60
4) Infiltration Rate			
	0.55	84.84	0.006
	0.45	83.77	-0.652

Incoming particle size distribution is input into the model using six particle size classes defined by particle diameters and their respective percent finer. As the coarser fraction increases in the sediment mixture greater trapping can be expected and conversely in the case of a larger fraction of fines. Finer particles are transported a greater distance through the filter and particles smaller in diameter than 0.004 mm are not expected to be trapped due to settlement. However, finer particles may be trapped in the filter due to infiltration. The model does reflect this trend of increased total trapping for a coarser distribution as compared to a finer distribution. The sensitivity for this parameter is given in Table II.7.4.

Increased rainfall on the filter and incoming runoff will increase the transportability of sediment down the filter, thus reducing the trapping efficiency (assuming the infiltration rate is constant). Moreover an increased runoff will also increase the flow velocity. The rainfall and runoff (incoming as well exiting) values were increased and decreased by 10% each and a decrease and increase in the predicted trapping efficiency was predicted as expected.

Sensitivity to Stochastic Parameter

The objective of this analysis was to determine the extent to which the stochastic distributions of channel density, flow rate and channel shape influence sediment trapping. This was accomplished by considering the randomness introduced by the stochastic distributions in predicted trapping and then determining the trapping when neglecting the randomness. This analysis was done on the validation model (Since in the general model the fitted distributions could not be neglected). Again data from plot four was considered for analysis.

The effect of randomness was determined by performing sensitivity analysis for six conditions which are

- *Case 1: Considering all distributions*
- *Case 2: Rill/channel density fixed*
- *Case 3: Rill/channel density and flow rate distribution fixed*
- *Case 4: Rill/channel density and W/D distribution fixed*
- *Case 5: Only flow rate distribution fixed*
- *Case 6: Only W/D distribution fixed*

For determining the sensitivity of the model to stochastic distributions, the distributions for channel density, flow rate, and W/D values were varied with other model parameters such as infiltration, runoff, Manning's roughness, etc., maintained at a constant base level. The influence of stochastic distributions may vary for

varying conditions of parameters such as infiltration. If infiltration in the filter is high and the deposition is primarily due to the high infiltration rate then the influence of these stochastic distributions will be restricted. On the other hand, if infiltration is low and high runoff occurs across the filter, then the way in which this surface flow is distributed across the filter and in the individual channels will have a greater effect on the sediment trapping.

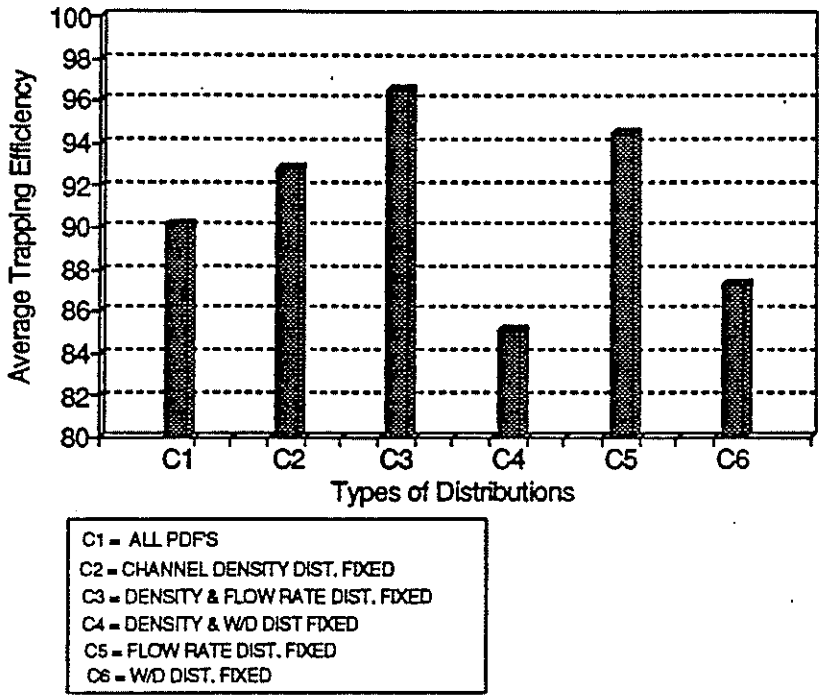

Figure II.7.26. Sensitivity of Model to Stochastic Distributions.

Conclusions on Sensitivity Analysis

Results indicate that the model is sensitive to physically based parameters such as Manning's n, ground slope, mean channel density, input particle size distribution and the runoff hydrograph. Sediment trapping can be expected to vary under different conditions of ground slope, roughness and runoff. Moreover as the slope increases appreciably a completely different stochastic distribution of channel densities and flow rates can be expected. Hence, to accurately predict and use the model for design purposes, correct values of the above parameters need to be input.

Sensitivity results also considered stochastic distributions of channel density and flow rates and compared them with the results obtained when neglecting randomness. Using the fitted distributions the model considers all the probable channel densities given the mean channel density and then determines the sediment trapping. This method is certainly an improvement over considering a single value of channel density (or uniform spacing of channels), a procedure used in most models.

Determination of rill/channel networks forming in grass filters is difficult, and thus stochastically representing them could be the best approach. Considering equal flow rates for all channels appreciably changes the sediment trapping and may not be the best approach towards representing the actual physical situation. Development of channels in grass filters generally does not start and proceed at the same rate. Some channels at their initial stages of development will have smaller flows and higher W/D values, and channels at a latter stage may have higher flows but lower W/D values hence, this variation in flows and shapes needs to be considered for determining the true trapping. The stochastic model attempts to do this.

Sensitivity analysis to input parameters was performed (except in the case of stochastic distributions) using the General model, developed to include the effect of rainfall on the filter trapping. As expected, the predicted trapping efficiencies were less than that predicted using the Validation model (neglecting the effect of rainfall). Sediment trapping under conditions of rainfall on the filter are reduced because greater volume of runoff is available to transport sediment down the filter. This effect was incorporated into the model. The other phenomenon that may reduce sediment trapping in the presence of rainfall, though to a lesser extent, is the resuspension of sediment (especially smaller sediment particles), which was not simulated in the General model.

CHAPTER II.8

SUMMARY, CONCLUSIONS AND RECOMMENDATIONS

Summary

Overland flow from upland fields has been observed to typically concentrate into channels as it passes through riparian vegetative filter strips. These filter strips, either constructed or naturally occurring, are utilized to filter sediment and nutrients from overland flow before it reaches the upland drainage channel or stream. Present models used to design constructed vegetative filter strips consider uniformly distributed shallow flow. In actual situations, especially on moderate to high slopes, the flow is rarely spread uniformly, hence the models overpredict the trapping capacity of natural filters. A model was needed to determine sediment trapping in vegetative filter strips considering channelization of flow. This research attempts to fulfill this objective.

Since occurrence of channels in the filter was random in nature it was decided to represent the channel network stochastically. Channel densities, channel flows and channel shapes were the three variables selected to represent the channel network. Probability density functions for these three variables were determined from data and by fitting standard distributions to the data. Deposition/detachment in each channel was modeled using physically based fundamental methods. Both these approaches were combined to determine the expected trapping for a given filter length subjected to a known storm event.

Field studies were performed to collect data required for development of model parameters and to evaluate the model. Studies were performed for vegetative filter strips comprised of fescue and sod and located on a average slope of 8.7%. Sediment laden runoff was generated by applying rainfall at a uniform constant intensity of 2.5 inches per hour for 2 hrs on a bare soil plot (conventional or no till). Runoff samples were collected at the entry and exit points to the filter. Surface topographic measurements of the filter were taken prior to and after each storm event run.

The actual probable channel network on the filter was generated using the DEM program. Further, based on the incoming surface runoff and the channel density flow distributions for the channels were determined. Using the topographic measurements, channel shapes at the beginning of the storm event were defined. Using the available data of channel density, flow rate distribution and channel shapes, standard distribution parameters were estimated. A Binomial distribution was fitted to the channel density data, and a Gamma distribution was fitted to the flow rate and channel shape (W/D) data. Model parameters used in the fundamental modeling were either determined from field experiments or estimated from literature.

Using the actual values of channel density for each of the individual filter plots and using probability density functions of flow rate and channel shape (W/D) generated from data, model validation was performed by comparing the predicted

sediment trapping to that observed during field runs. Validation runs were performed for Manning's n values of 0.2, 0.3, 0.35 and 0.40. Predicted trapping efficiencies were found to be within 2% of the observed values for a Manning's n of 0.35 for most of the filters, suggesting that the model has validity.

Comparison was also made of predicted and observed instantaneous maximum sediment flows and the sediment yield from the filter indicating a good agreement between the two. This comparison indicates that the model predictions are accurate.

Sensitivity analysis for the model was then performed using probability density functions generated from fitted distributions and considering dilution effects of rainfall on the filter. Sensitivity analysis was performed for discretization parameters, parameters used in the fundamental methods and the stochastic distributions.

Conclusions

Based on this study the following conclusions are made:

1. Experimental observations confirmed the fact that flow in naturally occurring riparian filters is typically channelized. Coarser particles were deposited primarily in the initial portion of the filter. Deposition over the period of the storm caused sediment deltas to form on the upslope portion of the filter which accentuated channelization. As sufficient deposition occurred in the filters bed load transport was also observed to occur in the channels.

2. The model predicted the expected trapping efficiencies within 2% of the observed values for a Manning's n of 0.35 for most of the filters, hence it can be said that the model has validity. Model estimates were particularly close for filters receiving runoff from a conventionally tilled area, which had higher sediment load compared to runoff originating from a no till area (which had a higher fraction of organic debris).

3. Comparisons of predicted and observed instantaneous exiting sediment flows and sediment yields indicated a good agreement, thus further confirming model validity.

4. Model predictions and field observations also indicated that sediment trapping efficiency did not proportionately increase for filter lengths beyond 15 ft under the given storm events and field conditions.

5. Prediction and observations also showed that sediment trapping for filters was reduced for subsequent storm events. This reduction could be attributed to the formation of sediment deltas in the filter from the prior event leading to increased channelization of flow. Sediment trapping due to infiltration played a major role in the total sediment trapping especially

for particles in the medium and finer range. This high infiltration may also have masked the effects of randomness of the channel networks.

6. The DEM model also performed well in simulating the channel network on the filter, except for the fact that partitioning of rills (observed on the field plots) was not simulated.

A sensitivity analysis indicates that:

7. Sediment trapping in the filters was observed to increase with the increase in the channel density.

8. As the roughness increased (which physically means a denser grass filter) sediment trapping of the filter increased.

9. Increase in the slope led to a coarser sediment distribution exiting the filter indicating reduced trapping.

10. Sensitivity analysis of the impact of randomness indicated that randomness did affect sediment trapping, hence a stochastic approach is an improvement over a deterministic one. Neglecting randomness of channel density (by introducing a spike equal to 1.0 at the mean channel density value) slightly increased the trapping efficiency. This indicated that the fitted distributions were biased towards a lower channel density than the mean. Neglecting randomness in case of flow rates (by introducing a spike at normalized flow of 1.0) caused a slight increase in trapping. This occurred as sediment load in the higher flow rate was higher (as total sediment load was partitioned in proportion of the flow rates) and thus greater sediment was trapped. In contrast, with randomness introduced, lower flow rates had higher probabilities and lower sediment load and thus predicted lower total trapping.

Recommendations for Further Research

Sediment trapping efficiencies using the model were determined for grass filters located on a uniform slope of 8.7 %. Hence the probability density functions for channel density, channel flow rates, and channel shapes were determined by fitting distributions to data applicable for a slope of 8.7 %. Investigations should be done to determine the changes in these distributions as the filter slope is increased or decreased. It is expected that as the filter slope is increased, channelization of flow will increase i.e, the distribution will shift toward lesser number of channels per unit width, greater flow rates in individual channels and deeper channel shapes. Exactly opposite trends might be expected for grass filters on lesser slopes. Based on such extensive investigations a data base could then be prepared which will help in future modeling efforts and subsequent design of riparian filter strips to be installed on upland drainage channels. Distributions of channel densities and channel shapes also

need to be determined with time as deposition occurs in the filter. With such distributions available a more dynamic approach to modeling could be achieved.

Further experimental observations need to be taken to determine the effect of rainfall on the filter on the trapping efficiency. Such observations would help to validate the general model developed in this research. Experimental observations need to be made to determine the infiltration rates in the grass filters and changes in them with time (storm duration). The model developed in this research also needs to be modified by incorporating a physically based prediction infiltration component. At the present the model assumes that infiltration occurs at a uniform rate down the filter and is equal to the difference between the inflow and outflow rates. An infiltration model needs to be added that will determine the changes in infiltration rate down the filter length and with time. The infiltration component also needs to take into account the effects of sediment deposition on the filter bed.

Laboratory scale measurements on natural grasses also need to be made to determine the effects of infiltration on deposition of sediment particles of different sizes. At present the model assumes that the change in particle size distribution as a result of infiltration is uniform, i.e, the fraction trapped due to infiltration is same for all particle sizes. This may not be the case, and that large sediment particles may have a greater possibility to be trapped compared to smaller particles due to infiltrating water. Analysis also needs to be done to determine the amount of deposition that needs to occur in grass filters such that bed load transport is initiated. This is assuming the methodology developed by Hayes (et al., 1979), that initially all the sediment reaching the bed is trapped (zone D), but as "sufficient" deposition occurs bed load transport is initiated.

Measurements need to be done to determine the critical tractive force for parent bed soil material covered with grass debris and tightly held together by grass roots. Such determinations may help in modeling detachment conditions in grass filters and also scour formation in grassed waterways and filters. Calibration runs are required to determine the changes in Manning's roughness for grass filter under different amounts of deposition. It is possible that the initial assumed Manning's roughness value for the filter may be different from its value after significant sediment deposition (this may be particularly true for filters that are not maintained).

Research also needs to be done for modeling of channel networks. Methods need to be developed such that bifurcation of rills/channels can be simulated (bifurcation of flow has been observed to occur in field conditions).

Finally, trial runs need to be made to determine whether the model can be extended to determine sediment trapping in riparian zones where a mixture of grasses, shrubs, trees and plant debris retard surface runoff in comparison to a uniform dense grass media found in vegetative filters strips.

REFERENCES

Abrahams, A.D. 1984. Channel Networks: A geomorphological prospective. Water Resources Research, 20(2): 161-168

Ackers, P. and W.R white. 1973. Sediment Transport: New Approach and Analysis. J. of Hydraulics Div. ASCE 99(HY11):2041-2060.

Barfield, B.J. 1992. Personal Communication. Department of Agricultural Engineering, University of Kentucky.

Barfield, B.J and M.C Hirschi. 1986. Tipping Bucket flow measurement on erosion plots. Transactions of the ASAE 29(6):1600-1604.

Barfield, B.J., R.I. Barnhisel., J.L Powell, M.C Hirchi and I.D Moore. 1984. Erodibilities and eroded size distribution of Wester Kentucky mine spoil and reconstructed topsoil. 1984. Symposium on Surface Mining, Hydrology, and Sedimentology and Reclamation. Pp. 179-189. University of Kentucky, Lexington, KY.

Barfield, B.J., and S. Albrecht. 1982. Field evaluation of the effectiveness of vegetative filters for controlling sediment from strip mines. Proceedings 1982 National Symposium on Surface Mine Hydrology, Sedimentology and Reclamation. College of Engineering, University of Kentucky, Lexington, KY.

Barfield, B.J., R.C Warner and C.T Haan. 1981. Applied Hydrology and Sedimentology for Disturbed Watersheds. Oklahoma technical Press, Stillwater, OK 74074

Barfield, B.J., I.D Moore and R.G Williams. 1979. Prediction of the sediment yield in surface mined watersheds. Proceedings Symposium on Surface Mining Hydrology, Sedimentology and Reclamation, University of Kentucky, Lexington, Kentucky. Pp. 89-92. December.

Clark, E.H., J.A Haverkamp and W. Chapman (eds.) Eroding Soils, 1985.

Dillaha, T.A. Water quality impacts of vegetative filter strips. 1989. ASAE Paper no. 89-2043.

Dillaha, T.A., J.H Sherrard., D. Lee., S. Mosthaghimi and V.O Shanoltz. 1988. Evaluation of vegetative filter strips as best management practices for feed lots. J. Water Poll. Cont. Fed. 60:1231-1238;1988.

Dillaha, T.A., R.B Reneau., S. Mosthaghimi., V.O Shanoltz and W.L Magette. 1987. Evaluating Nutrient and Sediment Losses from Agricultural Lands:vegetative filter strips. Annapolis, MD. USEPA. CBP/TRS 4/87.

Dillaha, T.A., J.H Sherrard and D.Lee. 1986. Long term effectiveness and maintenance of vegetative filter strips. Blacksburgh, VA.Virginia Water Resources Research Center. VPI-VWRRC-BULL 153.

Flanagan, D.C., G.R Foster., W.H Neibling and J.P Burt. 1989. Simplified equations for filter strip design. Transactions of the ASAE. Vol. 32(6):2001-2007.

Foster, G.R. 1986. Understanding ephemeral gully erosion. Pp. 90-125. In: Soil Conservation - Assessing the National Resources Inventory, Volume II. National Academy Press. 314 pp.

Foster, G.R., J.M. Gregory, L.D Meyer and C.K Multcher. 1985a. Revised contour subfactor values for the universal soil loss equation. Unpublished manuscript prepared for the background document for the revised USLE.

Foster, G.R and L.J lane. 1983. Erosion by concentrated flow in farm fields. Pp. 9.65-9.82. In Proceedings of the D.B Simons Symposium on Erosion and Sedimentation. Colarado State University, Fort Collins, CO.

Foster, G.R. 1982. Modeling the erosion process. PP.297-380. In C.T Haan (ed). Hydrologic Modeling of Small Watersheds. Monograph no. 5. ASAE St. Joseph. MI.

Foster, G.R., L.J. Lane, J.D. Nowlin, J.M. Laflen, and R.A. Young. 1980. A model to estimate sediment yield from field sized areas: Development of the model. In CREAMS - a field scale model for Chemicals, Runoff and Erosion from Agricultural Management Systems. USDA Conservation Research Report n. 26.

Foster, G.T., L.D Meyer and C.A Onstad. 1977b. A runoff erositivity factor and variable slope length exponents for soil loss estimates. Transactions of the ASAE 20(4):683-687.

Foster, G.R and L.D Meyer. 1975. Mathematical Simulation of Upland Erosion by Fundamental Erosion Mechanics. In Present and Prospective Technology for Predicting Sediment Yields and Sources. ARS-S-40. USDA Agricultural Services. Pp. 190-207.

Foster, G.R and L.D Meyer. 1972. A closed for soil erosion equation for upland areas. In Sedimentation (Einstein). H.W Shen (ed). Colarado State University, Fort Collins, CO. Chapter 12.

Hayes, J.C., B.J Barfield and R.I Barnhisel. 1984. Performance of grass filters under Laboratory and Field conditions. Transactions of the American Society of Agricultural Engineers 27(5):1321-1331.

Hayes, J.C and J.E Hairston. 1983. Modeling the long term effectiveness of vegetative filters as on-site sediment controls. ASAE Paper no. 83-2081. St. Joseph, MI.

Hayes, J.C., B.J Barfield and R.I Barnhisel. 1982. The use of grass filters for sediment control in strip mine drainage. Vol. III. Empirical verification of the procedures using real vegetation. Report no. IMMR82/070, Institute for Mining and Minerals Research, University of Kentucky, Lexington, KY.

Hayes, J.C. 1979. Evaluation of design procedures for vegetal filtration of sediment flowing water strips. A thesis presented to the University of Kentucky in partial fulfillment of the requirements for the degree of Doctor of Philosophy. Lexington, KY.

Hayes, J.C., B.J Barfield and R.I Barnhisel. 1979. Filtration of the sediment by simulated vegetation II. Unsteady flow with non-homogenous sediment. Trans of the ASAE 22(5):1063-1067.

Heatwole, C.D., T.A Dillaha and Saeid Mostaghimi. 1991. Agricultural BMP's applicable to Virginia. Department of Agricultural Engg. VPI & SU. Blacksburg. Virginia Water Resources Bulletin. VPI-VWRRC-BULL 169. 1991.

Hirschi, M.C. and B.J Barfield. 1988a. KYERMO- A physically based research erosion model Part I. Model development. Transactions of the ASAE 31(3):804-813.

Hirschi, M.C. and B.J Barfield. 1988b. KYERMO- A physically based research erosion model Part II. Model Sensitivity analysis and testing. Transactions of the ASAE 31(3):814-820.

Hirschi, M.C. 1985. Modeling soil erosion with emphasis on steep slopes and the rilling process. A thesis presented to the University of Kentucky in partial fulfillment of the requirements for the degree of Doctor of Philosophy. Lexington, KY.

Howard, A.D. 1971. Simulation of Stream Networks by headwall growth and branching. Geogr. Anal., 3:29-50.

Jenson, S,K and J.O Dominique. 1988. Extracting Topographic structure from digital elevation data for geographic information system analysis. Photogrammetric Engineering and Remote Sensing 54(11):1593-1600.

Karlinger, M.R and B.M Troutman. 1989. A random spatial network model based on elementary postulates. Water Resources Research, 25(5):793-798.

Laurensen, E.M. 1958. Total sediment load of streams. J. Of Hydraulics Div., ASCE, 84(HY1):1530-1,1530-36.

Lane, L.J and M.A Nearing. 1989. (eds). USDA - Water Erosion Prediction Project: Hillslope Profile Documentation. NSERL Report no. 2, USDA-ARS National Soil Erosion Laboratory, West Lafayatte, IN.

Law, A.M, and S.G. Vincent. 1983. UNIFIT - An interactive computer package for fitting probability distributions to observed data.

Leopold, L.B., M.G Wolman and J.P Miller. 1964. Fluvial Processes in Geomorphology. W.H Freeman and Co. 522 pp.

Lewis, S.M. 1991. PRORIL- A probabilistic Physically based erosion model. A thesis presented to the University of Kentucky in partial fulfillment of the requirements for the degree of Master of Science. Lexington. KY.

Lowrance, R.R., J.K Sharpe and J.M Sheridian. 1986. Long term sediment deposition in the riparian zone of a coastal plain watershed. L. Soil. Water. Conser., 41:266-271.

Mantz, P.A. 1977. Incipient transport in fine grains and flakes buy fluids-extended Shield's Diagram. Jour. of Hydraulics. Div. ASCE, 103 (HY6):601-615.

Meyer, L.D., G.R Foster and S. Nikolov. 1975. Effect of flow rate and canopy on rill erosion. Transactions of the ASAE 18(5):905-911.

Meyer, L.D and E.J Monke. 1965. Mechanics of soil erosion by rainfall and overland flow. Transactions of the ASAE. 8(4):572-577, 580.

Meyer, L.D and W.H Wischmeier. 1969. Mathematical simulation of the process of soil erosion by water. Transactions of the ASAE. 12(6):754-758, 762.

Moore, I.D., M.C Hirschi and B.J Barfield. 1983. Kentucky rainfall Simulator. TRANSACTIONS of the ASAE 26(4): 1085-1089.

Mossaad, M.E and T.H Wu. 1984. A stochastic model of soil erosion. International Journal for Numerical and Analytical Methods in Geomechanics 8:201-224.

Morisawa, M. 1985. Rivers:Form and Processes. Longman, New York.

Neibling, W.H and E.E Alberts. 1979. Composition and yield of soil particles transported through sod strips. ASAE paper no. 79-2065. ASAE, St. Joseph, MI.

Storm, D.E., G.O Brown, M.D Smolen, and R.L Huhnke. 1992. Effects of poultry litter on surface water quality-- part 2. Runoff results and analysis. ASAE Paper no. 922136. St. Joseph, MI:ASAE.

Storm, D.E. 1991. Modeling Dynamic Rill Networks from random surfaces on moderate slopes. A thesis presented to the University of Kentucky in partial fulfillment of the requirements for the degree of Doctor of Philosophy. Lexington, KY.

Storm, D.E., B.J Barfield., S.M. Lewis and A.W Fogle. 1990. A digital elevation model for defining microrelief drainage networks. ASAE Paper n. 90-2643. ASAE. St. Joseph. MI.

Tollner, E.W., B.J Barfield and J.C hayes. 1982. Sedimentology of erect vegetal filters. Journal of Hydraulics Division, American Society of Civil Engineers. 108(hy12):1518-1531.

Tollner, E.W., J.C Hayes and B.J Barfield. 1978. The use of grass filters for sediment control in strip mine drainage. Vol I. Theoretical Studies on artificial media. Report no. IMMR 35-RRR2-78. Institute for Mining and Minerals Research, University of Kentucky, Lexington, KY.

Tollner, E.W., B.J Barfield., C. Vachirakornwatana and C.T Haan. 1977. Sediment Deposition patterns in simulated grass filters. Transactions of the ASAE 20(5):940-944.

Tollner, E.W., B.J Barfield., C.T Haan and T.Y Kao. 1976. Suspended sediment filtration capacity of simulated vegetation. Transactions of the ASAE 19(11):678-682.

Wilson, L.G. 1967. Sediment removal from flood water by grass filtration. Transactions of the ASAE. vol. 10(1):35-37.

Yalin, M.S. 1963. An expression for bedload transportation. Jour. of the HYdr. Div., ASCE, 89(HY3):221-250.

Yang, C.T. 1973. Incipient Motion and Sediment Transport. Jour. of Hydr. Div., ASCE. 99(HY10):1805-1826.